

1 **Quantification of the contribution of the Beauce's Aquifer**  
2 **Groundwater Aquifer contribution to the discharge of the**  
3 **Loire River/River Loire discharge using thermal infrared**  
4 **satellite thermal infrared imagery imaging**

5  
6 **E. Lalot<sup>1</sup>, F. Curie<sup>12</sup>, V. Wawrzyniak<sup>23</sup>, F. Baratelli<sup>3</sup>, S.**  
7 **Schomburgk<sup>44</sup>, N. Flipo<sup>3</sup>, H. Piegay<sup>25</sup>, F. Moatar<sup>16</sup>**

8 [1,2,6]{ Laboratoire GEHCO, UFR sciences et techniques, Université François Rabelais,  
9 Tours, France }

10 [23,5]{ Plateforme ISIG, CNRS-UMR 5600 EVS, Ecole Normale Supérieure de Lyon,  
11 Université de Lyon, Lyon, France }

12 [4]{ ~~Dir. Eau Environnement et Ecotechnologies, Bureau de Recherches Géologiques et~~  
13 ~~Minières (BRGM), Orléans, France }~~ [3]{ Centre de Géosciences – Systèmes hydrologiques et  
14 Réservoirs, Mines ParisTech, Fontainebleau, France }

15 [4]{ Dir. Eau Environnement et Ecotechnologies, Bureau de Recherches Géologiques et  
16 Minières (BRGM), Orléans, France }

17  
18 Correspondence to: E. Lalot (eric.lalot@gmail.com)

19  
20 **Abstract**

Mis en forme : Anglais (États-Unis)

Mis en forme : Anglais (États-Unis)

21 Seven Landsat Thermal InfraRed (TIR) images, taken over the period 2000-2010, were used  
22 to establish longitudinal temperature profiles of the middle Loire River, where it flows above  
23 the Beauce aquifer. The groundwater discharge along the River course was quantified for each  
24 identified groundwater catchment areas using a heat budget based on the temperature variations  
25 of the Loire River temperature variations, estimated from the TIR images. The rResults showed  
26 that 75% of the temperature differences, between *in situ* observations and TIR image based  
27 estimations, remained within the  $\pm 1^{\circ}\text{C}$  interval. ~~The groundwater discharge along the River~~  
28 ~~course was quantified for each identified groundwater catchment areas using a heat budget~~  
29 ~~based on the Loire River temperature variations, estimated from the TIR images.~~ The main  
30 discharge area of the Beauce aquifer into the Loire River was located between river kilometers  
31 630 and 650, with where there was a temperature drop of around  $1^{\circ}\text{C}$  to  $1.5^{\circ}\text{C}$  in the summer  
32 and a temperature rise of about  $0.5^{\circ}\text{C}$  in winter. According to the heat budgets, groundwater  
33 discharge was higher during the winter period ( $13.5\text{ m}^3\cdot\text{s}^{-1}$ ) than during the summer period ( $5.3$   
34  $\text{m}^3\cdot\text{s}^{-1}$ ). These findings are in agreement with the results of both a groundwater budget and  
35 a process-based distributed hydrogeological model. Groundwater input was also found to be  
36 higher during the Loire's flow recession periods/ receding flow periods of the Loire River. This  
37 result confirms what was obtained using a groundwater budget and spatially locates  
38 groundwater input within the Middle sector of the Loire River. According to the heat budgets,  
39 groundwater discharge is higher during winter period ( $13.5\text{ m}^3/\text{s}$ ) than during summer ( $5.3$   
40  $\text{m}^3/\text{s}$ ). Groundwater input is also higher during the flow recession periods of the Loire River.

Mis en forme : Soulignement

## 42 1 Introduction

43 Water temperature is a key factor for aquatic fauna (Ward, 1992; Caissie, 2006). For instance,  
44 it controls oxygen's dissolution, a key parameter essential for aquatic organisms. River

45 temperature is controlled by many factors such as solar radiation, air temperature or  
46 groundwater discharge (Webb and Zhang, 1997, 1999; Hannah et al., 2004). However,  
47 quantifying the respective influence of these factors is often difficult, since temperature profiles  
48 of the river course have first to be established.

49 Since the late 1990's Thermal Infrared images (TIR) have been used to determine river water  
50 temperature along sections ranging from tens to hundreds of kilometers (Torgersen et al., 2001;  
51 Handcock et al., 2006 and 2012). Until now, TIR these images of water courses have mainly  
52 been used to: i) to identify cold refuges for fish in the summertime (Belknap and Naiman, 1998;  
53 Torgersen et al., 1999; Tonolla et al., 2010; Monk et al., 2013); ii) to study the thermal  
54 variability of rivers or alluvial floodplains and locate areas of similar thermal characteristics  
55 (Smikrud et al., 2008; Tonolla et al., 2010; Wawrzyniak et al., 2012, 2013); iii) to validate river  
56 temperature models (Boyd and Kasper, 2003; Cristea and Burges, 2009).

57 However, Most of these studies have been based on airborne TIR images, while Studies  
58 based on satellite TIR satellite images are scarce, mostly mainly due to their poor because the  
59 spatial resolution of these images is usually poor. In the case of the Landsat 7 satellite, one pixel  
60 of the TIR image represents 60\*60 m on the ground surface. Therefore, only a few large river  
61 courses could can be studied using TIR satellite images, as it is usually considered that it was  
62 considered that the river width had to must exceed 3 images pixels to allow enough accuracy  
63 to provide an accurate estimation of water temperature estimation (Handcock et al., 2006;  
64 Wawrzyniak et al., 2012). However, the advantage of Landsat satellite images have the  
65 advantage over airborne images is that they are of being freely available at different dates, so  
66 that providing archives are available to explore inter-annual or seasonal patterns. As the surface  
67 are ground covered by one a single satellite image would take time require a long time to be

68 covered ~~using air transportation~~by air, longitudinal thermal profiles derived from TIR satellite  
69 images also show less bias due to change in water temperature during sampling time.

70 ~~Although it has been shown that~~ Groundwater discharge ~~has already been shown may to~~ have  
71 a significant influence on surface water temperature (Hannah et al., 2004; Webb and Zhang,  
72 1997, 1999), ~~however,~~ this influence has seldom been studied ~~based on using~~ TIR images  
73 (Loheide and Gorelick, 2006; Burekholder et al., 2007; Wang et al., 2008, Danielescu et al.,  
74 2009; Mallast et al., 2014). Only one paper describes a test to quantify the groundwater  
75 discharge in a small stream, based on the longitudinal temperature profile established from ~~the~~  
76 airborne TIR images (Loheide and Gorelick, 2006). To ~~the authors' our~~ knowledge,  
77 groundwater discharge ~~into~~ rivers has ~~not never~~ been observed or quantified ~~before,~~ using  
78 satellite TIR images.

79 ~~The knowledge of Locating~~~~The location of~~ groundwater discharge areas ~~location is crucial to~~  
80 ~~assess the vulnerability of aquatic fauna, as these~~groundwater discharge locations can act as  
81 ~~sheltered areas (Belknap and Naiman, 1998).~~ ~~Understanding water temperature variations~~  
82 ~~Along along~~ the middle Loire River, where several nuclear power plants are located, ~~the~~  
83 ~~understanding of the water temperature evolution variations~~ is an operational issue for  
84 “Electricité De France” (EDF). ~~It has been shown that,~~For example, between the nuclear power  
85 plants of Dampierre and Saint – Laurent des Eaux, the Loire ~~River~~ temperature ~~has been shown~~  
86 ~~to be is~~ influenced by the groundwater discharge from the Beauce aquifer and the Val d’Orléans  
87 hydrogeological system (Alberic and Lepiller, 1998; Alberic, 2004; Moatar and Gailhard,  
88 2006). The average discharge of the Beauce aquifer ~~has already been was previously~~ quantified  
89 using hydrogeological numerical modelling (Monteil, 2011; Flipo et al., 2012) and ~~it~~ was found  
90 to ~~be eire~~have an ~~inter annual average of approximately~~  $10 \text{ m}^3 \cdot \text{s}^{-1} \text{ m}^2/\text{s}$  ~~on inter annual average.~~  
91 However, until now, ~~field measurement data has not been used to accurately locate or quantify~~

92 the groundwater discharge ~~has not been well located or quantified based on field measurement~~  
93 ~~data~~.

94 The main ~~goals-aims~~ of this study were ~~therefore~~ to test the ~~abilities-ability~~ of Landsat satellite  
95 thermal infrared images ~~from the Landsat satellite~~ i) to accurately determine water temperature  
96 in ~~a river having with~~ a width ~~under of less than~~ 180 m; ii) to characterize the ~~evolution~~  
97 ~~longitudinal and temporal variations~~ of temperature along a 135 km section of the middle Loire  
98 River overlying the Beauce aquifer between Dampierre and Blois; iii) to locate and quantify  
99 the ~~contribution of the Beauce aquifer~~ groundwater discharge's ~~contribution of the Beauce~~  
100 ~~aquifer~~ into the Loire River.

101

## 102 2 Study area

103 The study site ~~is-was~~ the Loire River between Gien and Blois (a 135 km reach), which overlies  
104 the Beauce aquifer (Figure 1). The catchment area of the Loire ~~River~~ at Gien is 35,000 km<sup>2</sup> and  
105 river slope is 0.4 m ~~/~~ km<sup>-1</sup> in the studied section (Latapie et al., 2014).

106 The river flow ~~rate~~ is measured daily in Gien, Orléans ~~-~~ and Blois, respectively at river  
107 kilometers 560, 635 and 695 (Banque HYDRO: www.hydro.eaufrance.fr). Over the 1964 ~~-~~ to  
108 2011 period, ~~in Orléans~~ the average flow ~~rate in Orléans is-was~~ 345 m<sup>3</sup>.s<sup>-1</sup>.m<sup>3</sup>/s, ~~and~~ the average  
109 flow ~~rates~~ in August ~~and January is-were~~ 95 m<sup>3</sup>.s<sup>-1</sup>.m<sup>3</sup>/s ~~and the average flow in January is-and~~  
110 553 m<sup>3</sup>.s<sup>-1</sup>.m<sup>3</sup>/s ~~respectively~~.

111 The width of the wet section of the middle Loire River ranges between 200 m and 450 m  
112 (Latapie et al., 2014), which is higher than the three image pixels ~~(180 m)-~~ threshold ~~(180 m)~~.  
113 However, during low flow periods, the Loire River ~~locally~~ forms several branches ~~locally~~ and  
114 the ~~river~~ main branch width can be as low as 50 m. During ~~low-flow~~ ~~these~~ periods, the average  
115 river depth is about 1 m in ~~this~~ ~~these sections~~ the studied reach. ~~The main weirs (natural and~~

Code de champ modifié

Mis en forme : Exposant

Mis en forme : Surlignage

116 ~~artificial) along~~Along the Loire River, the main natural and artificial weirs are located at river  
117 kilometers 571, 603, 635, 661, and 670, where the ~~river~~ water level shows a drop of just over 1  
118 m ~~at during~~ low flow periods.

119 ~~On~~The climate of the study area ~~the climate~~ is temperate. The mean annual air temperature in  
120 Orléans is 11°C. The cold season lasts from mid-November to early March, with an average air  
121 temperature of 4.0°C (data from Météo France at Orléans station for the period 1961-1990).  
122 The warm season lasts from late May to early September, with an average air temperature of  
123 17.2°C.

124 The water temperature of the Loire River is influenced by several factors: i) atmospheric heat  
125 fluxes from direct solar radiations, diffuse solar radiation, latent heat exchange, conduction and  
126 water emitted radiations; ii) groundwater discharge from the Beauce aquifer and Val d'Orléans  
127 hydrosystem (Alberic, 2004; Gutierrez and Binet, 2010);- iii) warm water originating from the  
128 cooling systems of the nuclear power plants of Dampierre and Saint-Laurent des Eaux (average  
129 discharge of 2 ~~m<sup>3</sup>.s<sup>-1</sup>.m<sup>2</sup>%~~ ~~by from~~ nuclear reactors). However, ~~the influence of~~ the nuclear  
130 power plants ~~only~~ ~~on~~ ~~have a slight influence on~~ the ~~Loire River~~ temperature of the river is low,  
131 as the cooling towers ~~the heat being~~ remove much of the ~~heat~~ ~~through~~ ~~cooling towers~~. The  
132 median temperature rise ~~of the Loire River~~ between the upstream and downstream sections  
133 of the nuclear power plants is 0.1°C with a 90<sup>th</sup> percentile of 0.3°C (Bustillo et al., 2014). The  
134 greatest increase in the Loire River temperature due to ~~the nuclear~~ power plants ~~in the Loire~~  
135 ~~River temperature~~ is observed in winter, ~~at during~~ low flow periods (<1°C); iv) ~~in~~ flows from  
136 the tributaries. The catchment area of the Loire River between Gien and Blois is around 5,600  
137 km<sup>2</sup>, (a 16% increase ~~of in~~ the ~~Loire River~~ catchment area over the 135 km reach). The influence  
138 of the tributaries on the ~~Loire River~~ river temperature is considered negligible in this section ~~of~~  
139 ~~the Loire River~~, since the water temperature of the tributaries is usually close to that of the Loire

140 ~~River itself temperature~~ (Moatar and Gailhard, 2006) ~~and the flow rates of the tributaries flows~~  
141 ~~are small~~ is low (less than  $1 \text{ m}^3 \cdot \text{s}^{-1}$ ). However, ~~in this section~~ the main tributary of the Loire  
142 ~~River in this section, is~~ the Loiret ~~River, which~~ drains water originating from both the Beauce  
143 aquifer and the Loire ~~River~~ (Alberic, 2004; Binet et al., 2011) and is very short (6 km). The  
144 influence ~~from of~~ the Loiret ~~River is therefore difficult to separate from~~ can therefore be  
145 ~~merged~~ included with that of the Beauce aquifer.

Mis en forme : Exposant

Mis en forme : Exposant

146

### 147 3 Material and methods

#### 148 3.1 Data

149 Seven satellite images from the Landsat 7 ETM+, presenting cloud cover under 10 %, were  
150 extracted from the period 1999-2010 (<http://earthexplorer.usgs.gov/>): (Table 1). ~~5~~ Five images  
151 were available in the warm season and ~~2~~ two in the cold season. They were taken at 12h30  
152 ~~(local hours)~~ LT in summer ~~time~~ and 11h30 ~~(local hours)~~ LT in winter ~~time~~. Each image covered  
153 the entire ~~course of the~~ Loire River ~~course~~ between Gien and Blois.

Mis en forme : Anglais (États-Unis)

Code de champ modifié

154 Water temperatures of the Loire River are monitored by EDF upstream of the nuclear power  
155 plant of Dampierre (river kilometer 571) and Saint-Laurent des Eaux (river kilometer 670) on  
156 an hourly basis. ~~In the cold season, t~~ The average ~~observed~~ daily water temperature ~~observed~~,  
157 on the days when the images were taken, was  $5.2^\circ\text{C}$  ~~in the cold season and~~  $23.7^\circ\text{C}$  ~~in~~ in the  
158 warm season, ~~it was~~  $23.7^\circ\text{C}$ .

159 River ~~discharge/~~ flow rates ~~flows~~ measured in Orléans, on the days the images were taken, were  
160 ~~comprised~~ between  $61 \text{ m}^3 \cdot \text{s}^{-1}$  ~~m<sup>3</sup>/s~~ and  $478 \text{ m}^3 \cdot \text{s}^{-1}$  ~~m<sup>3</sup>/s~~. On ~~6~~ six out of the ~~7~~ seven dates ~~for~~  
161 ~~which the images were taken~~, the Loire River ~~flow~~ ~~discharge/~~ flow rate was lower than the  
162 ~~average mean annual~~ flow.

163 **3.2 From the TIR satellite TIR images to the the Loire River longitudinal**  
164 **temperature longitudinal profiles of the Loire River**

165 ~~The first step was to locate pixels corresponding to TIR image pixels corresponding solely to~~  
166 ~~water only pixels. To do so this end, were first identified using~~ a threshold based on the TM 8  
167 band of the Landsat images (0.52 to 0.9  $\mu\text{m}$ ; USGS, 2013) ~~was used and~~ ~~only pixel~~-values  
168 below the threshold were kept. The aerial images in the visible range from ~~BD~~ the Ortho  
169 ~~database, from of~~ the “Institut National de l’information Géographique et forestière” (IGN),  
170 were used to set the threshold value for each image by comparing the TM 8 band to the Loire  
171 water course in ~~places where it was~~ known locations and ~~where it did~~ not altered with time. The  
172 Carthage database from the IGN, which maps all the French watercourses ~~in the form of as~~ lines,  
173 enabled ~~the further separation of~~ the water pixels belonging to the Loire River to be separated  
174 from ~~the pixels on those~~ belonging to other water bodies. As shade resulting from the clouds  
175 merges with the water pixel, it was removed manually using the same TM 8 band. The main  
176 advantage of using the TM8 band to detect water is that its the spatial resolution of the TM8  
177 band (15 m) is much higher than the spatial resolution that of the TM 61 band (60 m resolution,  
178 subsampled at 30 m; 10.4 to 12.5  $\mu\text{m}$ ) that which is used to estimate water temperature.

179 ~~In a~~ previous study (Handcock et al. 2006), ~~it was found~~ demonstrated that river temperatures  
180 should be estimated using only pure water pixels (~~i.e. that are water pixels situated more than a~~  
181 ~~pixel away separated~~ from the river banks by at least another water pixel). However, in the case  
182 of the middle Loire River, pure water pixels it was not possible to find could not be found pure  
183 water pixels along the entire river course, especially at low flow rates. Therefore, all water  
184 pixels were kept ~~but~~ Pixels composed of land and water were considered as land pixels.

185 In order to detect the water pixels from the TM 61 infrared band, a neighborhood analysis was  
186 therefore conducted, based on the water and land pixels already identified from the TM 8 band.  
187 Only pixels from the TM 61 band situated further than 60 m away from the already identified

Mis en forme : Non Surlignage



188 land pixels (using the TM 8 band) were kept. To detect pure water pixels, a 120 m buffer zone  
189 was used.

190 ~~The~~The temperature was then calculated for these identified Loire pixels from the radiance  
191 values extracted from the TM61 band of the Landsat images ~~(10.4 to 12.5  $\mu$ m)~~ using Planck's  
192 law (Chander et al., 2009). A value of 0.98 was used for ~~the~~ water emissivity. No atmospheric  
193 correction was taken into account, considering the fact that since the study area was included in  
194 a single LANDSAT image and that atmospheric conditions were homogeneous within the study  
195 area (underwith less than 10% of cloud cover). Finally, temperature values ~~for~~ these pixels  
196 were projected orthogonally on the longitudinal profile of the Loire ~~River~~ extracted from the  
197 Carthage database. The average temperature ~~was then for 200m long~~ averaged by sections ~~of~~  
198 200 m in length ~~was then calculated.~~ This A distance of 200 m ~~value~~ was chosen to be ~~so that~~  
199 it is similar ~~close from~~ to the width of the Loire River ~~width.~~ After this, a moving average  
200 ~~over for~~ 10 consecutive temperature values along the water course (2 km) was ~~further~~  
201 ~~conducted~~ calculated to smooth the temperature profile.

202 The temperature profiles extracted from the TIR images were then exploited in two different  
203 ways: i) the accuracy and uncertainty of the temperatures estimated from the TIR images was  
204 tested ~~through~~ by comparing them ~~comparison~~ with the hourly *in situ* measurements  
205 conducted by EDF at Dampierre and Saint-Laurent des Eaux; ii) a heat budget method, based  
206 on the temperature estimated from the TIR images, was used along successive sections of the  
207 Loire River ~~in order~~ to quantify the groundwater discharge for each section. The rResults were  
208 then compared with the ~~inter-annual~~ groundwater discharge ~~(period 1998-2007)~~ calculated by  
209 using a deterministic process-based groundwater budget method model applied over the whole  
210 Loire River basin. Calculated groundwater discharge estimations were compared over

211 successive groundwater catchment areas along the Loire River corresponding to the respective  
212 River sections.

213 **3.3 Groundwater discharge estimation - ~~heat~~Heat budget based on TIR images**

214 The middle Loire River was divided into 11 sections, so that ~~on~~for each section there was only  
215 one groundwater catchment area on each side of the river. The groundwater catchment areas  
216 were delineated using available piezometric maps, or elevation data (surface water catchment  
217 area) when the piezometric maps were missing. A dDescription of the method can be found in  
218 Schomburgk et al. (2012). The first section begins at river kilometer 560 where the flow rate is  
219 known-measured (Gien). The groundwater discharge was estimated on each section using a heat  
220 budget based on the temperatures derived from the TIR images.

221 The heat budget equilibrium can be written as (Moatar and Gailhard, 2006):

222  $\rho \cdot C \cdot Q_{i-1} \cdot T_{i-1} + F_{net} \cdot S + \rho \cdot C \cdot Q_{gw} \cdot T_{gw} = \rho \cdot C \cdot Q_i \cdot T_i$  \_\_\_\_\_ (1)

223  $Q_{i-1} + Q_{gw} = Q_i$  \_\_\_\_\_ (2)

224 The groundwater discharge in the section ( $Q_{gw}$ ) can be deduced:

225  $\frac{\rho \cdot C \cdot Q_{i-1} \cdot (T_{i-1} - T_i) + F_{net} \cdot S}{\rho \cdot C \cdot (T_i - T_{gw})} = Q_{gw}$  \_\_\_\_\_ (3)

226  $Q_{i-1}$  [ $m^3 \cdot s^{-1}$ ] is the upstream flow rate of the section at ~~the~~ temperature  $T_{i-1}$  [ $^{\circ}C$ ],  $Q_i$  [ $m^3 \cdot s^{-1}$ ] is  
227 the downstream flow rate of the section at ~~the~~ temperature  $T_i$  [ $^{\circ}C$ ].  $Q_{gw}$  [ $m^3 \cdot s^{-1}$ ] is the  
228 groundwater flow rate at ~~the~~ temperature  $T_{gw}$  [ $^{\circ}C$ ]. ~~At~~For each section, the flow entering the  
229 section is equal to the flow entering the previous section plus the groundwater discharge  
230 estimated over the previous section (only taken into account if the estimated discharge ~~is~~was  
231 positive). The groundwater temperature was considered to be 12.6°C in summer and 12.1°C in  
232 winter, based on 292 measurements from the ADES database (www.ades.eaufrance.fr)

Mis en forme : Anglais (États-Unis)

Mis en forme : Anglais (États-Unis)

Mis en forme : Anglais (États-Unis)

Mis en forme : Anglais (États-Unis)

Mis en forme : Anglais (États-Unis)

Mis en forme : Anglais (États-Unis)

Mis en forme : Anglais (États-Unis)

Mis en forme : Anglais (États-Unis)

Mis en forme : Anglais (États-Unis)

Mis en forme : Anglais (États-Unis)

Mis en forme : Anglais (États-Unis)

Mis en forme : Anglais (États-Unis)

Mis en forme : Anglais (États-Unis)

Mis en forme : Anglais (États-Unis)

Mis en forme : Anglais (États-Unis)

Mis en forme : Anglais (États-Unis)

Mis en forme : Anglais (États-Unis)

Mis en forme : Anglais (États-Unis)

Mis en forme : Anglais (États-Unis)

Mis en forme : Anglais (États-Unis)

Mis en forme : Anglais (États-Unis)

Mis en forme : Anglais (États-Unis)

Mis en forme : Exposant

Mis en forme : Exposant

Mis en forme : Anglais (États-Unis)

Mis en forme : Anglais (États-Unis)

Mis en forme : Anglais (États-Unis)

Mis en forme : Anglais (États-Unis)

Mis en forme : Anglais (États-Unis)

Mis en forme : Anglais (États-Unis)

Mis en forme : Anglais (États-Unis)

Mis en forme : Anglais (États-Unis)

Code de champ modifié

233 ~~conducted in the vicinity of the Loire River, over the 1991-2011 period~~  $\ominus$ . Over 80% of the  
 234 ~~temperature measurements were comprised~~ included in the interval ~~mean~~ ~~mean plus~~ plus or  
 235 ~~minus +1.4°C~~ ~~mean minus~~ means.  $F_{net}$  [W.m<sup>-2</sup>] stands for the atmospheric heat fluxes and S  
 236 [m<sup>2</sup>] is the surface area covered by the Loire River on the section. S was estimated ~~by adding~~  
 237 ~~up~~ for each section ~~by adding~~ the ~~surfaces~~ surface areas of all the water pixels identified on the  
 238 satellite images ~~from the TM 61 band~~. ~~It is~~ This value was therefore ~~probably somewhat~~  
 239 underestimated, as images pixels composed of both water and land ~~are not considered~~ were not  
 240 ~~included~~, but tests on some Loire River sections showed that this underestimation did not  
 241 ~~exceed 20%~~.  $\rho$  is the water density [kg.m<sup>-3</sup>] and C [J.kg<sup>-1</sup>.K<sup>-1</sup>] is the ~~water~~ specific heat of  
 242 water.

Mis en forme : Anglais (États-Unis)

Mis en forme : Exposant

Mis en forme : Anglais (États-Unis)

Mis en forme : Exposant

Mis en forme : Exposant

243 The heat fluxes ( $F_{net}$ ) between the Loire River and the atmosphere ~~were~~ was estimated as  
 244 follows (Salencon and Thébault, 1997; Chapra, 1997; Table 2):

Mis en forme : Anglais (États-Unis)

Code de champ modifié

$$245 \quad F_{net} = RA + RS - RE - CV - CE \quad (4)$$

Mis en forme : Anglais (États-Unis)

246 Where RA is ~~the~~ atmospheric radiations, RS ~~the~~ solar radiations, RE ~~the~~ emitted radiations, CV  
 247 the conduction, and CE the condensation/evaporation.

248 The atmospheric parameters extracted from the SAFRAN database from Météo France  
 249 (Quintana-Segui et al., 2008) were averaged along the successive Loire River sections  
 250 ~~considered in the study~~. ~~Every~~ All the atmospheric factors ~~was~~ were averaged over the 24 h  
 251 period preceding the ~~taking acquisition~~ of the infrared image. This choice is questionable as the  
 252 water temperature in the Loire River may be influenced by changes in atmospheric factors over  
 253 a longer time period. However, ~~water~~ the travel time of water between Gien and Blois ~~is~~ was  
 254 ~~about~~ between 1 to 1.5 days on the dates when the images were taken. Atmospheric parameters  
 255 ~~should~~ were therefore not ~~be~~ integrated over a period exceeding a day.

256 As the Loire River course is large, no shading from the alluvial forest was taken into  
257 account.

### 258 **3.4 Groundwater discharge estimation - ~~groundwater~~ Groundwater** 259 **budget modeling**

260 ~~Average groundwater discharge into the Loire River was calculated using groundwater budget~~  
261 ~~per groundwater catchment areas over the 1998-2007 period. Effective rainfall was then~~  
262 ~~calculated for each catchment area using Turc formulae. The useable ground reserves are~~  
263 ~~available at the municipality scale and 1000 weather stations were considered in order to~~  
264 ~~spatialize the atmospheric parameters. Effective rainfall was further separated between~~  
265 ~~infiltration to the groundwater and surface runoff using the IDPR index (Mardhel et al., 2004;~~  
266 ~~Putot and Bichot, 2007). Known groundwater withdrawals, obtained from the Water Agencies,~~  
267 ~~were then removed from the calculated infiltrated water. In steady state condition, the average~~  
268 ~~infiltration rate in the aquifers corresponds to the groundwater discharge into the Loire River.~~

269 The Eau-Dyssée model was used to determine the groundwater discharge along the Loire River.

270 Eau-Dyssée is an integrated, distributed, process-based model that allows the simulation of the  
271 main components of the water cycle in a hydrosystem. Detailed descriptions of the model can  
272 be found in Flipo et al. (2012) and Saleh et al. (2011). This model has been applied to basins of  
273 different scales and hydrogeological settings, e.g., the Oise basin (4,000 km<sup>2</sup>; Saleh et al., 2011),  
274 the Rhône basin (86,500 km<sup>2</sup>; Habets et al., 1999; Etchevers et al., 2001), the Seine basin  
275 (65,000 km<sup>2</sup>; Ledoux et al., 2007; Pryet et al., 2015) and the Loire basin (120,000 km<sup>2</sup>; Monteil,  
276 2011).

277 Eau-Dyssée ~~conceptually~~ divides a hydrosystem ~~conceptually~~ into three interacting  
278 compartments: a surface, an -unsaturated zone and a saturated zone. Specifically, the model  
279 couples different modules, which simulate the mass balance of surface water ~~mass balance~~, the

Mis en forme : Interligne : Double

Mis en forme : Police :

280 runoff, the river flow rate/discharge, the fluctuations of in-stream water levels~~fluctuations~~, the  
281 flow rate in the unsaturated and saturated zones.

282 The water fluxes  $q_{sa}$  [ $m^3 \cdot s^{-1}$ ] at the stream-aquifer interface are~~is~~ computed ~~with~~using a  
283 conductance model, i.e., they are~~it~~ is proportional to the difference between the piezometric  
284 [m], and the in-stream water level,  $h_r$  [m], i.e.:

Mis en forme : Non Exposant/ Indice

$$285 \quad q_{sa} = k_{riv}(h_g - h_r) \quad (5)$$

Mis en forme : Police :

286 Where the proportionality constant  $k_{riv}$  [ $m^2 \cdot s^{-1}$ ] is the conductance of the stream-aquifer  
287 interface. Rushton (2007) showed that the main factor controlling this coefficient is the  
288 horizontal hydraulic conductivity  $k_H$  [ $m \cdot s^{-1}$ ] of the underlying aquifer.

$$289 \quad k_{riv} = f k_H L \quad (6)$$

290 Where  $f$  [-] is an adjustable correction factor, generally ranging between 0.9 and 1.2 (Rushton,  
291 2007), and  $L$  [m] is the length of the river in the aquifer mesh.

292 Eau-Dyssée was applied to the Loire basin by Monteil (2011). In-stream water levels were  
293 assumed to be constant. This work has been improved by simulating the time variability of in-  
294 stream water levels with a Manning-Strickler approach (Chow, 1959). Under the assumptions  
295 that the river section is rectangular and that its width is much greater than its depth,  $h_r$  is given  
296 by:

$$297 \quad h_r = b + \left( \frac{Q}{\alpha \kappa W S^{1/2}} \right)^{5/3} \quad (7)$$

Mis en forme : Police :

298 Where  $b$  [m] is the riverbed elevation,  $Q$  [ $m^3 \cdot s^{-1}$ ] is the discharge,  $\alpha = 1 \text{ m}^{1/3} \cdot s^{-1}$ ,  $\kappa$  [-] is the  
299 Strickler's coefficient,  $W$  [m] is the river width,  $S$  [-] is the slope of the riverbed.

300 Details on the input data and model calibration can be found in Monteil (2011). The  
301 morphological parameters of the Loire River (river width and riverbed elevation and slope)

were estimated from several cross sections surveyed with an average spacing of 1.6 km (Latapie et al., 2014). The Strickler's coefficient was calibrated against observed hydrographs at six stations along the Loire River, three of which are located on the Beauce aquifer.

The stream-aquifer exchanges were simulated in the period 1996-2013 at a daily time step for the river network at a 1 km resolution. Groundwater discharge was then calculated for the 11 Loire River sections selected for the heat budget.

### 3.5 Uncertainty estimation – Heat budget

Equation (3) was used to estimate the uncertainty associated with the calculated groundwater discharge. The absolute uncertainty of the calculated groundwater discharge  $\Delta Q_{gw}$  can be computed as:

$$\Delta Q_{gw} = \left| \frac{\rho \cdot C \cdot (T_{i-1} - T_i)}{\rho \cdot C \cdot (T_i - T_{gw})} \right| \cdot \Delta Q_{i-1} + \left| \frac{\rho \cdot C \cdot Q_{i-1}}{\rho \cdot C \cdot (T_i - T_{gw})} \right| \cdot \Delta(T_{i-1} - T_i) + \left| \frac{F_{net}}{\rho \cdot C \cdot (T_i - T_{gw})} \right| \cdot \Delta S + \left| \frac{(\rho \cdot C \cdot Q_{i-1} \cdot (T_{i-1} - T_i) + F_{net} \cdot S)}{\rho \cdot C \cdot (T_i - T_{gw})^2} \right| \cdot \Delta(T_i - T_{gw}) \quad (8)$$

$\Delta Q_{i-1}$  is the absolute uncertainty in the river flow rate. A 10% uncertainty in the flow estimation is considered:  $\Delta Q_{i-1} = 0.1 \cdot Q_{i-1}$ .

$\Delta(T_{i-1} - T_i)$  is the absolute uncertainty in the river temperature variations over the corresponding river section. It is computed, based on the known spatial variation between Dampierre and Saint-Laurent des Eaux of the shift difference disparity between the temperature estimated from the TIR images and the temperature estimated from in-situ measurements. At each date, a shift difference disparity by river kilometers and finally then by river sections was calculated. The value of this shift difference disparity was added to  $T_i$  to estimate the variation in surface water temperature that could be caused by uncertainties in the measurements:

$$(T_{i_{new}} - T_i)$$

Mis en forme : Titre 2

Mis en forme : Police : (Par défaut) Times New Roman, 12 pt, Couleur de police : Noir

Mis en forme : Non Surlignage

Mis en forme : Non Surlignage

Mis en forme : Non Surlignage

Mis en forme : Non Surlignage

324  $\Delta(T_{i-1} - T_i) = |(T_{i-1} - T_{i_{new}}) - (T_{i-1} - T_i)|$  \_\_\_\_\_ (10)

325  $\Delta S$  is the absolute uncertainty in the water surface estimate. It ~~is~~ was computed based on the  
326 difference between the water surface estimated from the TM 61 band and from the TM 8 band  
327 of the Landsat satellite.  $\Delta S$  was calculated at each date for every study section of the Loire  
328 River sections (11 sections).

329  $\Delta(T_i - T_{gw})$  is the absolute uncertainty of the difference between the river temperature and the  
330 groundwater temperature. It ~~is~~ was considered to be equal to 2°C in order to take into account  
331 both groundwater temperature variability and surface water temperature accuracy.

## 333 4 Results

### 334 4.1 Temperature accuracy and temperature uncertainty

335 Temperature accuracy is the average difference between the temperature estimated from the  
336 TIR images and the temperature measured in-situ (Handcock et al., 2012). The comparison  
337 between the *in situ* and TIR derived temperatures shows that, on average, the TIR images tend  
338 to overestimate the Loire River water temperature in winter (+ 0.3°C) and to underestimate it  
339 in summer (- 1°C).

340 Over 75% of the TIR derived temperatures ~~are were comprised~~ between  $\pm 1^\circ\text{C}$  of the  
341 temperature measured directly ~~into~~ the river (11 times out of 14; Figure 2). ~~But However,~~ the  
342 temperature difference ~~exceeds exceeded~~  $1.5^\circ\text{C}$  on 29/05/2003 and on 29/07/2002 at the  
343 Dampierre station and on 29/07/2002 at Saint-Laurent des Eaux.

344 Temperature uncertainty can be ~~associated~~linked to the repeatability of the measurement  
345 (Handcock et al., 2012). The study of the longitudinal ~~evolution~~changes of the difference  
346 between TIR images based temperature and in-situ measurements may give ~~some~~ ideas

Code de champ modifié

347 ~~about~~ of the degree of ~~uncertainty~~ (Figure 2). On average, the variation in temperature  
348 ~~difference~~ ~~variation~~ ~~remained~~ below 0.8°C over the 100 km reach from Dampierre- to Saint-  
349 Laurent-des-Eaux, except on the 29/07/~~th~~ of July 2002 (1.3°C) and on the 29/05/~~th~~ of May 2003  
350 (2.3°C). The variation of the temperature difference ~~is~~ ~~was~~ ~~comprised~~ between 0.0004°C.km<sup>-1</sup>  
351 and 0.02°C.km<sup>-1</sup> (mean of 0.007°C.km<sup>-1</sup>).

Mis en forme : Exposant

352  
353 ~~Tests were carried out~~ ~~To~~ ~~to~~ assess the influence of the nature of the water pixels (pure or non-  
354 pure) ~~on the estimated temperature~~, ~~tests were carried out~~. For the 200-m long sections of the  
355 Loire River ~~In the case where, for a 200 m long section of the Loire River,~~ pure water pixels  
356 exist, temperature was estimated for both pure ~~water pixels~~ and non-pure water pixels. ~~The~~ ~~A~~  
357 linear regression ~~was conducted for between the~~ temperature estimated with pure water pixels  
358 and ~~temperature that~~ estimated with non-pure water pixels ~~was drawn~~, and the standard  
359 ~~deviation of the residuals of the regression line was calculated~~. The standard deviation is found  
360 ~~to be comprised between 0.18°C and 0.21°C and the slope of the regression line is comprised~~  
361 ~~between 0.98 and 1.01~~. Taking into account the data from all the dates, the slope of the  
362 regression line is 1, while it is 0.98 ~~when summer alone is considered~~ ~~summer only~~ and 0.72  
363 ~~considering for winter only~~ ~~alone~~ (Figure 3a; Figure 3b). The difference between the  
364 temperatures estimated from pure and non-pure water pixels ~~usually~~ ~~generally~~ ~~remained~~ in the  
365 ~~+/-0.5°C interval (over 98% of the time), which corresponds to the approximate resolution of~~  
366 ~~the satellite sensors~~. Therefore, taking into account non-pure water pixels does not seem to  
367 ~~induce an important~~ ~~cause a large~~ bias in the case of the Loire River.

Mis en forme : Soulignement

368 However, when the number of water pixels in a 200-m section of the Loire River decreases  
369 ~~(small~~ ~~due to the river being narrower~~ ~~river width~~), the standard deviation of the observed  
370 temperature increases notably (

Code de champ modifié



371 Table 3). Peak temperature values along the longitudinal ~~temperature/thermal~~ profile may  
372 appear in places where the main river branch is particularly narrow. This phenomenon is mostly  
373 due to the uncertainties inherent ~~to~~in the satellite sensor. Uncertainty ~~is~~can be reduced by  
374 averaging and as the number of. ~~The more~~ pixels ~~are~~ considered over a section increases, ~~the~~  
375 ~~lower~~ the uncertainty decreases. ~~The moving average over 2 km that which was applied to~~  
376 the data is was therefore useful in lowering/reducing the uncertainty.

Mis en forme : Soulignement

#### 378 4.34.2 Longitudinal temperature profiles

379 Among the ~~7~~seven longitudinal temperature profiles, ~~3~~three main profile types can be  
380 observed: ~~2~~two in summer~~time~~ and one in winter~~time~~.

381 In summer~~time~~, a mean decrease ~~of~~in the temperature between 0.8°C and 1.5°C can be  
382 observed on all the profiles between ~~the~~ river kilometers 620 and 650. A local temperature  
383 minimum is observed on every profile at river kilometer 645, close to ~~the town~~ La Chapelle-  
384 Saint-Mesmin. The ~~river~~ temperature ~~increases~~increased again from river kilometer 660 to 680  
385 and then ~~remains~~remained constant or ~~decreases~~decreased once more after river kilometer 680.

386 However, the temperature profiles differ between river kilometers 560 and 620, since the water  
387 temperature ~~can~~ either increased (29/05/2003 and 19/07/2010; ~~Figure 3~~Figure 4b) or decreased  
388 (24/08/2000, 29/07/2002 and 20/08/2010; ~~Figure 3~~Figure 4a).

Code de champ modifié

Code de champ modifié

Code de champ modifié

389  
390 Figure 3**b**). Another difference appears between river kilometers 650 and 660, with either a  
391 temperature drop (29/05/2003 and 19/07/2010) or a temperature rise (29/07/2002). Then, from  
392 river kilometers 680 to 700 the temperature dropped ~~can appear~~ downstream of~~after~~ river

393 kilometer 690 (29/05/2003, 19/07/2010 and 20/08/2010), or ~~upstream of~~ river kilometer  
394 690 (24/08/2000 and 29/07/2002) and ~~be then was~~ followed by a rise in the temperature.

395 In winter ~~time~~ the temperature ~~tends-tended~~ to increase sharply ~~by around 0.5°C~~ between river  
396 kilometers 630 and 650 ~~by around 0.5°C~~ (Figure 4a).

Code de champ modifié

397 ~~Sharp temperature changes in the longitudinal profile need to be compared with the uncertainty~~  
398 ~~and not with the accuracy. The sharpest temperature changes observed on the longitudinal~~  
399 ~~profiles are were comprised between 0.04°C.km<sup>-1</sup> and 0.1°C.km<sup>-1</sup> (mean of 0.074°C.km<sup>-1</sup>). The~~  
400 ~~sharpestmost marked~~ temperature changes are therefore at least one order of magnitude higher  
401 ~~than those changes that are to be~~ expected from the uncertainty (0.0072°C.km<sup>-1</sup>). They are  
402 therefore likely to be meaningful in terms of physical processes.

#### 403 **4.44.3 Groundwater discharge estimation - Heat ~~and groundwater~~ budget and** 404 **groundwater modeling**

405 The groundwater discharge ~~is was~~ estimated at ~~7~~ ~~seven~~ dates (winter and summer) along the  
406 same successive ~~11 sections of the Loire River sections~~, using ~~respectively the both~~ heat budget  
407 ~~and groundwater modeling two methods~~ (Figure 5a). ~~We found that~~ ~~the variability of the~~  
408 ~~with the heat budget is was~~ much higher than ~~that the variability of the groundwater discharge~~  
409 ~~estimated using groundwater modeling (with respective maximum standards deviations of 0.6~~  
410 ~~m<sup>3</sup>.s<sup>-1</sup>.km<sup>-1</sup> and 0.11 m<sup>3</sup>.s<sup>-1</sup>.km<sup>-1</sup> respectively)~~. Nevertheless, the modeled groundwater  
411 ~~discharge always stay was always with-in~~ the interval estimated by the heat budget. Overall,  
412 ~~compared to the groundwater modeling, the heat budget tend sed~~ to overestimate the  
413 ~~groundwater discharge between river kilometers 640 and 660 in winter and to underestimate~~  
414 ~~the discharge it~~ between river kilometers 660 and 680 in summer (Figure 5b; Figure 6a; Figure  
415 ~~6b).~~

Code de champ modifié

416 High groundwater discharge rates (~~0.3155~~  $\text{m}^3 \cdot \text{s}^{-1} \cdot \text{km}^{-1}$ ) on average ~~are were~~ calculated with the  
417 ~~groundwater heat~~ budget method between river kilometers 563 and 565 and they also showed  
418 a noticeable increase in the standard deviation ( $0.6 \text{ m}^3 \cdot \text{s}^{-1} \cdot \text{km}^{-1}$ ). ~~It corresponds to a section~~  
419 ~~where the groundwater discharge, estimated using the river heat budget, shows a noticeable~~  
420 ~~increase in the standard deviation ( $0.6 \text{ m}^3 \cdot \text{s}^{-1} \cdot \text{km}^{-1}$ )~~. However, these high discharge rates and  
421 high standard deviation were not observed using the groundwater modeling.

422 Between river kilometers 570 and 630, the average estimated groundwater discharge using both  
423 methods is low (~~respectively less than~~  $0.3 \text{ m}^3 \cdot \text{s}^{-1} \cdot \text{km}^{-1}$ ) and less than  $0.1 \text{ m}^3 \cdot \text{s}^{-1} \cdot \text{km}^{-1}$   
424 respectively) and the standard deviation it shows was also low standard deviation (~~respectively~~  
425 ~~less than~~  $0.4 \text{ m}^3 \cdot \text{s}^{-1} \cdot \text{km}^{-1}$ ) and less than  $0.05 \text{ m}^3 \cdot \text{s}^{-1} \cdot \text{km}^{-1}$  respectively).

426 Further downstream, according to both methods, the groundwater discharge ~~shows showed~~ a  
427 marked peak in the section located between river kilometers 630 and 660. At river kilometer  
428 640, the groundwater discharge estimated with the heat budget ~~is was~~ positive at each date  
429 (~~comprised~~ between  $0.3$  and  $1.5 \text{ m}^3 \cdot \text{s}^{-1} \cdot \text{km}^{-1}$ ) and it also ~~corresponds corresponded~~ to the  
430 location where the groundwater discharge ~~is was~~ maximum maximal according to the  
431 groundwater ~~budget method modeling~~ (between  $0.65$  and  $0.9 \text{ m}^3 \cdot \text{s}^{-1} \cdot \text{km}^{-1}$ ). Both methods  
432 showed a high The standard deviation of the groundwater discharge is high according to both  
433 methods (~~respectively~~  $0.4$  and  $0.1 \text{ m}^3 \cdot \text{s}^{-1} \cdot \text{km}^{-1}$  respectively).

434  
435 ~~From river kilometers 640 to 690, the standard deviation of the estimated discharge is~~  
436 ~~comprised between~~  $0.4$  and  $0.5 \text{ m}^3 \cdot \text{s}^{-1} \cdot \text{km}^{-1}$ , which is higher than between river kilometers 560  
437 ~~and 630~~. For river kilometers 660 to 680 the results of the two methods give were different.  
438 results from river kilometers 660 to 680 with a negative discharge estimated by the heat budget

439 ~~(-0.24 m<sup>3</sup>.s<sup>-1</sup>.km<sup>-1</sup> on average) and a positive discharge calculated by groundwater modeling~~  
440 ~~(0.12 m<sup>3</sup>.s<sup>-1</sup>.km<sup>-1</sup> on average).~~

441 Negative flow values ~~are were~~ estimated ~~by using~~ the heat budget method. Theoretically, the  
442 estimated groundwater discharge should not be negative. However, in summer~~time~~, negative  
443 discharge values are ~~especially~~ computed when water temperature increases but when this  
444 increase cannot be explained by ~~the~~ atmospheric heat fluxes. In winter~~time~~, negative discharge  
445 values can also be obtained when water temperature shows a decrease that cannot be explained  
446 by ~~the~~ atmospheric heat fluxes.

447 ~~The absolute uncertainty in the groundwater discharge estimated by the heat budget remaineds~~  
448 ~~underbelow 0.4 m<sup>3</sup>.s<sup>-1</sup>.km<sup>-1</sup> overfor more than 75% of the time. Taking into account the~~  
449 ~~uncertainty, we found that in the Loire River section between river kilometers 636 and 645 at~~  
450 ~~all the dates the estimated groundwater discharge was always above 0.03 m<sup>3</sup>.s<sup>-1</sup>.km<sup>-1</sup> in the~~  
451 ~~Loire River section comprised between river kilometers 636 and 645 the estimated groundwater~~  
452 ~~discharge remains at all dates over 0.03 m<sup>3</sup>.s<sup>-1</sup>.km<sup>-1</sup> and iswas therefore significant. On this river~~  
453 ~~section, the groundwater discharge estimated with the heat budget is comprisedwas between~~  
454 ~~2.8 m<sup>3</sup>.s<sup>-1</sup> and 13.7 m<sup>3</sup>.s<sup>-1</sup>, while the groundwater dischargethat estimated throughusing~~  
455 ~~groundwater modeling variesd between 5.2 m<sup>3</sup>.s<sup>-1</sup> and 8.6 m<sup>3</sup>.s<sup>-1</sup>.~~

Mis en forme : Exposant

Mis en forme : Exposant

Mis en forme : Exposant

Mis en forme : Exposant

## 458 5 Discussion

### 459 5.1 Temperature accuracy ~~and temperature uncertainty~~

460 There are many factors that can contribute to the ~~accuracy or to the uncertainty uncertainty~~ of  
461 the temperature estimation using ~~the TIR satellite TIR~~ images. ~~Main sources of uncertainty~~

462 ~~come from~~The main factors are the satellite sensors, the atmospheric influence on the  
463 transmitted radiation~~s~~ (Kay et al., 2005; Chander et al., 2009; Lamaro et al., 2013), the change  
464 in water emissivity with time and along the water course, the existing correlation between  
465 radiation~~s~~ estimated at neighboring pixels (Handcock et al., 2006) and the thermal stratification  
466 of water temperature (Robinson et al., 1984; Cardenas et al., 2008). The TIR images only  
467 measure the temperature ~~from of of~~ the upper 100 µm of the water body (skin layer), which may  
468 differ from the temperature ~~from of of~~ the entire water body (Torgersen et al., 2001).

469 The average difference between the temperature estimated from the ~~TIR~~ satellite ~~TIR~~ images  
470 and the ~~temperature one~~ observed *in situ* ~~is was~~  $-0.51^{\circ}\text{C}$ . On average, it is found that  
471 temperature estimated using TIR images tends to underestimate real water temperature.

472 ~~However, t~~The opposite ~~phenomenon~~ has ~~also regularly~~ been ~~regularly~~ observed, ~~using TIR~~  
473 ~~satellite images with this method~~. Wawrzyniak et al. (2012) found that TIR images  
474 overestimated~~d~~ the Rhône River temperature by  $+0.5^{\circ}\text{C}$  on average. Another study was  
475 conducted over several water courses of the Pacific Northwest rivers of the United States  
476 (Handcok et al., 2006). A ~~mean temperature difference of~~  $+1.2^{\circ}\text{C}$  ~~mean temperature difference~~  
477 was found, when the water course width was over three image pixels and ~~a of~~  $+2.2^{\circ}\text{C}$  ~~mean~~  
478 ~~temperature difference~~ when the width was ~~comprised~~ between 1 and 3 pixels. ~~A m~~Mean  
479 temperature differences ~~of comprised~~ between  $+1^{\circ}\text{C}$  and  $+1.9^{\circ}\text{C}$  ~~was were also~~ found in  
480 ~~another~~ four ~~other~~ Pacific Northwest rivers ~~of the United States~~ (Cherkauer et al., 2005).

481 ~~N~~However, negative biases were also found (Barsi et al., 2003). In the case of Lake Tahoe, the  
482 temperature estimated with TIR images was on average ~~1.5°C to 2.5°C~~ colder ~~by 1.5°C to 2.5°C~~  
483 than the temperature observed *in situ*. Similar results were observed on the Wenatchee River ~~of~~  
484 ~~in~~ the United States (Cristea and Burges, 2009).

485 Satellite based TIR images can therefore lead to either ~~underestimation-under-~~ or over-  
486 estimation of the water temperature. Depending on the time of the year, ~~the-this~~  
487 ~~disparity/difference shift~~ can ~~happen be either positive or negative in both directions~~ (Lamaro  
488 et al., 2013, De Boer, 2014).

Mis en forme : Surlignage

Mis en forme : Surlignage

489 Findings from this study confirm that ~~water temperature can be either over- or under-estimated~~  
490 ~~using TIR images the TIR images can lead to either overestimation or underestimation of the~~  
491 ~~water temperature~~ (Figure 2). The biggest ~~disparity shift~~ ~~was~~ observed on the 29/07/2002,  
492 when the water temperature ~~is-was~~ maximum ( $> 26^{\circ}\text{C}$ ) and the flow ~~rate~~ minimum ( $60 \text{ m}^3 \cdot \text{s}^{-1}$   
493  ~~$\text{m}^3/\text{s}$~~   $- 1.33 \text{ l} \cdot \text{s}^{-1} \cdot \text{km}^{-2}$ ). One possible explanation of this ~~shift~~ would be that high ~~water~~  
494 evaporation at this date leads to a low ~~temperature of water skin surface~~ ~~temperature water~~.

Mis en forme : Surlignage

Code de champ modifié

Mis en forme : Surlignage

495 The average temperature difference between TIR images and *in situ* measurements ~~is-was~~  
496 similar to ~~what had been that~~ observed in ~~the~~ previous studies (Handcock et al., 2006;  
497 Wawrzyniak et al., 2012), even though in this study non-pure water pixels ~~are-kept~~ ~~were~~  
498 ~~included~~ and no atmospheric correction ~~is-was~~ applied. Temperature estimation using non-pure  
499 water pixels from TIR images may therefore be more robust than ~~is-previously~~  
500 ~~considered usually thought~~. However, this study also shows that differences between  
501 temperatures estimated using TIR images and temperatures observed *in situ* may locally exceed  
502  $2^{\circ}\text{C}$ .

503 The temperature estimated for non-pure water pixels could be influenced by the temperature  
504 ~~from~~ of the riverbanks. However, tests ~~that were~~ carried out show that the difference in  
505 temperatures estimated using TIR images or measured *in situ* cannot be explained only by the  
506 bias resulting from the use of the non-pure water pixels. Uncertainty resulting from the satellite  
507 sensors low resolution can also play a role, ~~particularly especially~~ in ~~narrow~~ parts ~~where of~~ the  
508 Loire River ~~which are~~ ~~is~~ particularly narrow.

509 **5.2 Longitudinal temperature profiles and groundwater discharge estimations**

510 TIR images of water courses have been used in the past to detect groundwater discharge areas  
511 and to differentiate them from hyporheic upwelling areas (Burekholder et al., 2007). The  
512 surface of the cold water plumes associated with groundwater upwelling has been shown to be  
513 correlated with the groundwater discharge rate (Danielescu et al., 2009). However, quantifying  
514 groundwater discharge using a river heat budget based on TIR images has only been done once,  
515 on a small stream (along a 1.7 km reach, with a flow of  $10 \text{ l s}^{-1}$ ) and using high precision aerial  
516 images (Loheide and Gorelick, 2006).

Mis en forme : Exposant

517 This work is new ~~in that~~ because firstly, groundwater discharge ~~is was~~ estimated on a large river,  
518 ~~based on~~ through satellite TIR satellite images and secondly the results were compared. ~~The~~  
519 ~~comparison with the groundwater discharge estimations obtained~~ using ~~a groundwater~~  
520 ~~budget~~ groundwater modeling, ~~over the successive catchment areas is also new, as~~ Loheide  
521 and Gorelick (2006), on the other hand, compared their findings with groundwater discharge  
522 estimated through measurements of the stream flow over successive stream cross sections. This  
523 last technique is difficult to use for large rivers and limited section lengths<sup>2</sup>, due to the  
524 ~~important~~ high uncertainty in flow rate measurements (up to 20 %).

525 There are several sources of uncertainty in ~~the~~ groundwater discharge estimation using the heat  
526 budget. First, there is ~~the an~~ uncertainty ~~coming from~~ in the estimation of water temperature  
527 water temperature estimation. ~~As a result, important uncertainties are attached to the estimated~~  
528 ~~groundwater discharge when the length of the river section considered is small, at the river~~  
529 ~~surface and of the river flow rate. In general in the present study, We found that the resulting~~  
530 uncertainty in groundwater discharge estimate remained mainly below  $0.4 \text{ m}^3 \cdot \text{s}^{-1} \cdot \text{km}^{-1}$ , which  
531 is quite high in case of low groundwater discharge. ~~Then, there~~ There are also uncertainties  
532 inherent ~~to in~~ the heat budget method used as f. Factors such as bed friction, heat conduction

Mis en forme : Exposant

Mis en forme : Exposant

Mis en forme : Exposant

533 through the river bed, or hyporheic exchange ~~are not considered~~are not included. However, for  
534 ~~that kind of~~ the type of slow flowing river studied, the influence of bed friction is assumed to  
535 be low, ~~especially~~ particularly in summer (Evans et al., 1998). Similarly, heat conduction  
536 through the bed usually plays a minor role in the ~~global~~ overall river heat budget (Hannah et  
537 al., 2008). The effect of heat conduction and hyporheic flows can be confused with the  
538 groundwater discharge, which probably leads to a small overestimation of the groundwater  
539 discharge. The ~~water travel~~ time for water to travel along the river is not taken into account in  
540 the heat budget either. As a result the river temperature tends to be slightly overestimated due  
541 to, the influence of the local atmospheric conditions ~~over the river temperature tends to be~~  
542 ~~slightly overestimated~~. There are also uncertainties ~~are also attached~~linked ~~to~~ using  
543 groundwater modeling to calculate the groundwater discharge ~~calculated using~~with the  
544 groundwater budget modeling. ~~Nevertheless, t~~The modeling of the Loire River flow in Blois,  
545 Orléans and Gien over the 1996-2013 period works well neverthelessprovided good results  
546 (Nash criteria of 0.98, correlation of 0.99 and relative bias of 0.01 m<sup>3</sup>.s<sup>-1</sup>). ~~Then, the~~  
547 ~~groundwater discharge estimate given by the groundwater budget method is an average value~~  
548 ~~over a 10 year period. In contrast, only 7 TIR images are taken into account in this study and~~  
549 ~~the average discharge estimated using these images is therefore related to the sampling date. It~~  
550 ~~may suffice to explain the difference between the average estimated groundwater flow using~~  
551 ~~the heat budget and the flow calculated by the groundwater budget method.~~ ~~DD~~espite all the  
552 uncertainties, the groundwater discharge estimated using the heat budget stays remained within  
553 the same order of magnitude ~~as~~of ~~the discharge that~~ calculated ~~with the groundwater~~  
554 ~~budget using groundwater modeling.~~ ~~At maximum, the groundwater discharge rate, estimated~~  
555 ~~with the heat budget, overestimates, or underestimates, by less than~~ It was always below ± 1  
556 m<sup>3</sup>.s<sup>-1</sup>.km<sup>-1</sup> of the discharge calculated by using the groundwater ~~budget~~modeling. The average  
557 groundwater discharge calculated by using ~~the groundwater budget~~groundwater modeling for

Mis en forme : Exposant

Mis en forme : Exposant

Mis en forme : Soulignement

Mis en forme : Non Exposant/ Indice



558 ~~the inter-annual period is was~~ always within the range of variation of the ~~groundwater~~ discharge  
559 estimated using the river heat budget. The shapes of the ~~average~~ estimated ~~average~~ groundwater  
560 discharge curve ~~provided by the two methods along the Loire River is also are also~~ relatively  
561 ~~close similar to the one calculated by the groundwater budget between the two methods~~  
562 (coefficient of determination  $r^2 = 0.782$ ).

563 On the upstream part of the Loire ~~River~~, i.e. from river kilometer 560 to 635, the groundwater  
564 discharge estimated from the heat budget ~~appears to be was~~ ~~small low~~ (less than  $0.3 \text{ m}^3 \cdot \text{s}^{-1} \cdot \text{km}^{-1}$ ;  
565 ~~Figure 5a~~), except for some dates around river kilometer 564. ~~It is known that~~ ~~This is possibly~~  
566 ~~explained by the fact that~~ ~~between river kilometers 610 and 625~~ the Loire River ~~loses loses~~ water  
567 through the Val d'Orléans karstic system ~~between river kilometers 610 and 625~~ (Alberic, 2004;  
568 Binet et al., 2011). ~~This is also consistent in line with the results from the groundwater modeling.~~  
569 ~~It should be noted that~~ The high standard deviation of the estimated discharge near river  
570 kilometer 564 ~~may could~~ be explained ~~not only~~ by ~~both~~ real variations ~~of in~~ the discharge rate,  
571 ~~as highlighted by the groundwater budget, but and also by the~~ bias resulting from the small  
572 length of the corresponding section. ~~Similarly, high groundwater discharge around river~~  
573 ~~kilometer 564 ( $0.6 \text{ m}^3 \cdot \text{s}^{-1} \cdot \text{km}^{-1}$ ) was also found by the BRGM, using a groundwater budget over~~  
574 ~~the successive groundwater catchment areas to calculate the average interannual groundwater~~  
575 ~~discharge over the period 1998-2007 (Schomburgk et al., 2012). A calculation of the average~~  
576 ~~interannual groundwater discharge along the Loire River, over the period 1998-2007, was also~~  
577 ~~carried out by the BRGM, using a groundwater budget over the successive groundwater~~  
578 ~~catchment areas (Schomburgk et al., 2012). They found similarly high groundwater discharge~~  
579 ~~around river kilometer 564 ( $0.6 \text{ m}^3 \cdot \text{s}^{-1} \cdot \text{km}^{-1}$ )~~

580 A first thermal anomaly appears downstream of river kilometer 620. From river kilometer 63~~65~~  
581 to river kilometer 645 the groundwater discharge estimated with the heat budget ~~is~~

Mis en forme : Exposant

Mis en forme : Exposant

Mis en forme : Exposant

582 ~~comprised~~was between 0.3 and 1.5 m<sup>3</sup>.s<sup>-1</sup>.km<sup>-1</sup>. ~~We found that, t~~Taking into account the  
583 ~~uncertainties, the groundwater discharge calculated by~~through the heat budget always  
584 ~~stay~~remained positive between river kilometers 636 and 645. This river section corresponds to  
585 a known discharge area of the Beauce aquifer and the Val d'Orléans hydrosystem (Desprez and  
586 Martin, 1976; Gonzalez, 1991; Binet et al., 2011) ~~that~~which is also identified by ~~the~~  
587 groundwater ~~budget~~modeling (calculated discharge ~~comprised~~was between 0.6 and 0.9 m<sup>3</sup>.s<sup>-1</sup>.  
588 km<sup>-1</sup>). Schomburgk et al. (2012) calculated a slightly lower, but still significant, groundwater  
589 ~~discharge of 0.5 m<sup>3</sup>.s<sup>-1</sup>.km<sup>-1</sup>.~~It is interesting to note that, along the Loire River, the maximum  
590 ~~estimated~~exchange rates ~~estimated~~occurred at times when ~~re~~the river flow ~~decreases~~decreased  
591 ~~over~~between two consecutive days, while the lowest exchange rate ~~is~~was estimated when the  
592 ~~river~~flow ~~increases~~increased (Figure 6Figure 7). ~~The m~~Maximum groundwater discharge ~~is~~  
593 ~~was~~ also estimated in winter (13.5 m<sup>3</sup>.s<sup>-1</sup> compared to 5.3 m<sup>3</sup>.s<sup>-1</sup> in summer), when ~~the~~  
594 groundwater level ~~was~~is at its highest. ~~It is consistent~~This is in line with the results from the  
595 ~~groundwater modeling showing~~which show an average discharge of 7.6 m<sup>3</sup>.s<sup>-1</sup> in winter~~time~~  
596 ~~and 6 m<sup>3</sup>.s<sup>-1</sup> in summertime.~~ It is known that temporal changes in river water levels can lead to  
597 ~~important~~large modifications in exchange rates and ~~exchange~~directions (Sophocleous, 2002).  
598 During a rise in ~~river~~the water level, water ~~from the river~~ can flow into the lateral aquifer while  
599 the opposite ~~phenomenon happens~~is true at ~~during~~ low ~~river~~flow rates. Thus, the variation in  
600 estimated exchange rates is likely to have a physical basis. An exchange rate of 11.5 to 12.5  
601 ~~m<sup>3</sup>.s<sup>-1</sup>~~m<sup>3</sup>.s<sup>-1</sup> was calculated at la Chapelle Saint-Mesmin (river kilometer 642), using geo-  
602 chemical tracers during the summer ~~of~~1986 (Gonzalez, 1991). ~~It is~~This was higher than the  
603 maximum groundwater discharge estimated in ~~the~~summer using the heat budget (7.5 m<sup>3</sup>.s<sup>-1</sup>).  
604 Therefore, the high discharge rates estimated using the heat budget are plausible. The ~~satellite~~  
605 TIR ~~satellite~~ images ~~allow to locate~~enable the main groundwater discharge area ~~to be located~~

Mis en forme : Exposant

Mis en forme : Exposant

Mis en forme : Exposant

Code de champ modifié

Mis en forme : Exposant

Mis en forme : Exposant

Mis en forme : Exposant

Mis en forme : Exposant

Mis en forme : Exposant

606 precisely, along the right bank of the Loire River and ~~2 the two~~ to ~~3 three~~ kilometers upstream  
607 ~~from of~~ the confluence with the Loiret (~~Figure 7~~Figure 8).

Code de champ modifié

608 On the downstream part of the Loire River, between river kilometers 650 and 680, ~~both heat~~  
609 ~~budget and groundwater modeling estimations showed a decrease in~~ groundwater discharge  
610 ~~decreases according to both estimations (heat budget and groundwater budget modeling). Over~~  
611 ~~the last 20 km downstream the heat budget would suggest a slight increase in the groundwater~~  
612 ~~discharge, in line. This is consistent with the findings from Schomburgk et al. (2012).~~  
613 ~~However~~On the other hand, ~~the groundwater modeling predicts a slight decrease in the~~  
614 ~~groundwater discharge. Then, downstream of river kilometer 680, groundwater discharge~~  
615 ~~estimated with the groundwater budget increases again. However, even though an increase in~~  
616 ~~the median discharge estimated with the heat budget is observed, its value stays negative~~

617 The change in the groundwater discharge rate ~~with over~~ time could explain why the river  
618 temperature ~~may~~ either ~~increased~~rise or ~~decreased~~drop between river kilometers 645 and 665,  
619 or between river kilometers 570 and 620. However, atmospheric factors are also likely to play  
620 a role, even though ~~the~~ atmospheric data available do not offer a satisfactory explanation for  
621 this phenomenon. The influence of warm water ~~discharges discharged~~ from the nuclear power  
622 plant on the longitudinal temperature profile ~~is was~~ not noticeable either, as no sudden  
623 temperature rise ~~is was~~ observed at the ~~locations of the~~ nuclear plants ~~locations~~. In the case of  
624 Saint-Laurent des Eaux, ~~discharged~~ warm water ~~discharges~~ may nevertheless contribute ~~for to~~  
625 ~~a certain extent some part~~ to the ~~global overall~~ temperature rise observed between river  
626 kilometers 670 and 680 (~~Figure 3~~Figure 4a; Figure 4b), ~~but however~~, the temperature rise ~~begins~~  
627 of the power plant.

Code de champ modifié

Code de champ modifié

628 Similarly, no sudden temperature variations could be explained by weirs across the river course  
629 ~~and or~~ changes in the river slope (~~less than 0.1°C change between the 1 km~~ a kilometer up- or

630 ~~downstream of the structure upstream and the 1 km downstream~~), although abrupt temperature  
631 changes near weirs have been observed on the Ain River in France (Wawrzyniak, 2012), based  
632 on airborne TIR images. This could be explained by the small reservoir capacity of the Loire  
633 River upstream of the weirs (Casado et al., 2013), and ~~also due to probably by~~ the low spatial  
634 resolution of the ~~TIR satellite TIR~~ images. ~~The Landsat images were also taken around 12h:30~~  
635 ~~LT and thermal stratification may could be expected to be more important greater later during in~~  
636 ~~the day.~~

## 638 6 Conclusion

639 Temperatures of the middle Loire River were estimated using Thermal InfraRed (TIR) Landsat  
640 images. ~~Although no atmospheric correction was implemented and non-pure water pixels were~~  
641 ~~taken into account With no atmospheric correction considered and taking into account non-pure~~  
642 ~~water pixels~~, temperature differences ~~between from~~ *in situ* observations and TIR images based  
643 estimations ~~s~~ remains within the interval defined in previous studies (i.e. 75% of these  
644 differences being in the  $\pm 1^\circ\text{C}$  interval). Therefore, this study shows that river temperature may  
645 be studied from ~~satellite TIR satellite~~ images even when ~~the~~ river width falls below the three-  
646 pixels<sup>2</sup> width threshold (i.e. < 180 m). However, the river temperature can be seriously  
647 underestimated at low flow ~~rates~~ and ~~when high~~ water temperatures ~~is high~~ (differences of over  
648  $2^\circ\text{C}$ ).

649 We demonstrate that groundwater discharge to a large river can be estimated using satellite  
650 images. The groundwater discharge was estimated along the Loire River using both ~~a the~~ heat  
651 budget based on the longitudinal temperature profiles established from the TIR images, and a  
652 groundwater ~~budget on the successive groundwater catchment areas~~ model. The  
653 ~~variation evolution~~ of the groundwater discharge rate along the Loire River ~~are is found to~~

Mis en forme : Soulignement

654 ~~be were~~ -similar ~~according to with~~ both methods. The main discharge area of the Beauce aquifer  
655 into the Loire River is located between river kilometers ~~6365~~-645 (close to la Chapelle Saint-  
656 Mesmin).

657 According to the TIR images, the average groundwater discharge between river kilometers 636  
658 and 645 appears to be higher in winter~~time~~ (~~13.5 m<sup>3</sup>.s<sup>-1</sup>~~) than in summer~~time~~ (~~13.5 m<sup>3</sup>.s<sup>-1</sup> and~~  
659 ~~5.3 m<sup>3</sup>.s<sup>-1</sup> respectively~~~~5.3 m<sup>3</sup>.s<sup>-1</sup> m<sup>3</sup>/s~~). ~~It is consistent~~This is in line with the results from the  
660 groundwater modeling- which showing an average discharge of 7.6 m<sup>3</sup>.s<sup>-1</sup> in winter~~time~~ and ~~6~~  
661 ~~m<sup>3</sup>.s<sup>-1</sup> in summer~~~~time~~. ~~It~~The groundwater discharge is-was also ~~found to be~~ higher when the  
662 ~~Loire River~~river flow ~~decreases~~-~~decreased~~ ~~between~~-over two consecutive days. Our TIR  
663 images ~~underline~~-highlight that instantaneous groundwater discharge can vary considerably s  
664 are highly variable with over time. Therefore, average discharge is not sufficient to predict the  
665 observed changes in water temperature along the river course.

666 To assess the consistency and robustness of the~~se~~ results, further studies could be conducted  
667 using more sophisticated model~~ing~~ of both the groundwater discharge and ~~the~~-stream  
668 temperature.

669

## 670 **Acknowledgements**

671 This work was part of the scientific program “Control factors of river temperature at regional  
672 scale in the Loire catchment” funded by European funds for regional development~~European~~  
673 ~~funds (FEDER, Fonds Européens de Développement Régional)~~, Etablissement Public Loire and  
674 the Loire River Basin authority (Agence de l’Eau Loire Bretagne). The calculation of  
675 groundwater fluxes using groundwater budget was also funded by Electricité De France (EDF)  
676 and monitored by Mohamed Krimissa from EDF.

Mis en forme : Expositant

677 We would like to thank Alain Poirel from EDF for the hourly Loire River temperature  
678 measurements on the days ~~of the~~ images were taken. We would also like to thank Météo France  
679 for the information from the SAFRAN database. ~~We are grateful to Nicolas Flipo and Fulvia~~  
680 ~~Baratelli from Mines Paris Tech for their helpful comments on our results. Finally, We we~~  
681 ~~finally thank are very grateful to the team of water~~ assessment and evaluation team of  
682 ~~knowledge on water~~ of the BRGM water ~~department and especially department, particularly~~  
683 Alexandre Brugeron, for their help in characterizing groundwater catchment areas and  
684 groundwater fluxes.

685 **References**

686 Alberic, P.: River backflooding into a karst resurgence (Loiret, France). *Journal of Hydrology*,  
687 286, 194-202, 2004.

688 Alberic, P. and Lepiller, M.: Oxydation de la matière organique dans un système hydrologique  
689 karstique alimenté par des pertes fluviales (Loiret, France), *Water Resources*, 32, 2051-2064,  
690 1998.

691 Barsi, J.A., Barker, J.L., and Schott, J.R.: An atmospheric correction parameter calculator for a  
692 single thermal band earth-sensing instrument. *In: Geoscience and Remote Sensing*  
693 *Symposium, IGARSS'03, Proceedings, IEEE International*, 21-25 July, Toulouse, 3014-3016,  
694 2003.

695 Belknap, W. and Naiman, R.J.: A GIS and TIR procedure to detect and map wall-base channels  
696 in Western Washington. *Journal of Environmental Management*, 52, 147-160, 1998.

697 Binet, S., Auterives, C., and Charlier, J.B.: Construction d'un modèle hydrogéologique d'étiage  
698 sur le val d'Orléans. rapport final. ICERE, Orléans, France, rapport final, 2011.

699 Boyd, M. and Kasper, B.: Analytical Methods for Dynamic Open Channel Heat and  
700 Mass Transfer: Methodology for Heat Source Model Version 7.0, Watershed Sciences  
701 Inc., Portland, Oregon, USA, 2003.

702 Burekholder, B.K., Grant, G.E., Haggerty, R., Khangaonkar, T., and Wampler, P.J.: Influence  
703 of hyporheic flow and geomorphology on temperature of a large, gravel bed river, Clackamas  
704 River, Oregon, USA. *Hydrological Processes*, 22, 941-953, 2007.

705 Bustillo, V., Moatar, F., Ducharne, A., Thiery, D., and Poirel, A.: A multimodel comparison  
706 for assessing water temperatures under changing climate conditions via the equilibrium

Mis en forme : Anglais (États-Unis)

707 temperature concept: case study of the Middle Loire River, France. *Hydrological Processes*,  
708 28, 1507-1524, 2014.

709 Caissie, D.: The thermal regime of rivers: a review. *Freshwater Biology*, 51, 1389-1406, 2006.

710 Cardenas, B., Harvey, J.W., Packman, A.I., and Scott, D.T.: Ground-based thermography of  
711 fluvial systems at low and high discharge reveals potential complex thermal heterogeneity  
712 driven by flow variation and bio-roughness. *Hydrological Processes*, 22, 980-986, 2008.

713 Casado, A., Hannah, D.M., Peiry, J.L., and Campo, A.M.: Influence of dam-induced  
714 hydrological regulation on summer water temperature: Sauce Grande River, Argentina. *Ecology*,  
715 6, 523-535, 2013.

716 Chander, G., Markham, B.L., and Helder, D.L.: Summary of current radiometric calibration  
717 coefficients for Landsat MSS, TM, ETM+ and EO-1 ALI sensors. *Remote Sensing of  
718 Environment*, 113, 893-903, 2009.

719 Chapra, S.C.: Surface Water-Quality Modeling. *Civil Engineering Series*, McGraw-Hill  
720 International editions, Singapore Civil Engineering Series, 1997.

721 Cherkauer, K.A., Burges, S.J., Handcock, R.N., Kay, J.E., Kampf, S.K., and Gillepsie, A.R.:  
722 Assessing satellite based and aircraft based thermal infrared remote sensing for monitoring  
723 pacific northwest river temperature. *Journal of the American Water Resources Association*, 41,  
724 Issue 5, 1149-1159, 2005.

725 Chow, V.T.: Open Channel Hydraulics, McGraw Hill Company Inc., New York, 1959.

726 Cristea, N.C. and Burges, S.J.: Use of thermal infrared imagery to complement monitoring and  
727 modeling of spatial stream temperatures. *Journal of Hydrologic Engineering*, 14, 1080-1090,  
728 2009.



729 Danielescu, S., MacQuarrie, K.T.B., and Faux, N.R.: The integration of thermal infrared  
730 imaging, discharge measurements and numerical simulation to quantify the relative  
731 contributions of freshwater inflows to small estuaries in Atlantic Canada. *Hydrological  
732 Processes*, 23, 2847-2859, 2009.

733 De Boer, T.: Assessing the accuracy of water temperature determination and monitoring of  
734 inland surface waters using Landsat 7 ETM+ thermal infrared images. *Master thesis, Delft  
735 University, Netherlands*, 2014.

736 Desprez, N. and Martin, C.: Inventaire des points d'eau - piézométrie et bathymétrie des  
737 alluvions du lit majeur de la Loire entre Saint-Hilaire Saint-Mesmin et Saint-Laurent des Eaux. *BRGM, Orléans, France, Rep. 76 SGN 461 BDP*, 1976.

739 [Etchevers, P., Golaz, C., and Habets, F.: Simulation of the water budget and the river flows of  
740 the Rhone basin from 1981 to 1994, \*Journal of Hydrology\*, 244, 60-85, 2001.](#)

741 Evans, E.C., McGregor, G.R., and Petts, G.E.: River energy budgets with special reference to  
742 river bed processes. *Hydrological Processes*, 12, 575-595, 1998.

743 Flipo, N., Monteil, C., Poulin, M., De Fouquet, C., and Krimissa, M.: Hybrid fitting of a  
744 hydrosystem model: Long-term insight into the Beauce aquifer functioning (France). *Water  
745 Resources Research*, 48, [W05509, doi:10.1029/2011WR011092](#), 2012.

746  
747 Gonzalez, R.: Étude de l'organisation et évaluation des échanges entre la Loire moyenne et  
748 l'aquifère des calcaires de Beauce. *Ph.D. thesis, Université d'Orléans, Orléans, France*, 1991.

749 Gutierrez, A. and Binet, S.: La Loire souterraine: circulations karstiques dans le val d'Orléans. *Géosciences*, 12, 42-53, 2010.

Mis en forme : Anglais (États-Unis)

Mis en forme : Anglais (États-Unis)

Mis en forme : Anglais (États-Unis)

751 [Habets, F., Etchevers, P., Golaz, C., Leblois, E., Ledoux, E., Martin, E., Noilhan, J., and Otlé,](#)  
752 [C.: Simulation of the water budget and the river flows of the Rhône basin, Journal of](#)  
753 [Geophysical Research, 104, 31145-31172, 1999.](#)

754 Hancock, R.N., Gillespie, A.R., Cherkauer, K.A., Kay, J.E., Burges, S.J., and Kampf, S.K.:  
755 Accuracy and uncertainty of thermal-infrared remote sensing of stream temperatures at multiple  
756 spatial scales. *Remote Sensing of Environment*, 100, 427-440, 2006.

757 Hancock, R.N., Torgersen, C.E., Cherkauer, K.A., Gillespie, A.R., Tockner, K., Faux, R.N.,  
758 and Tan, J.: Thermal infrared sensing of water temperature in riverine landscapes. *Fluvial*  
759 *Remote Sensing for Science and Management*, First Edition. Carbonneau P.E. and Piégay H.  
760 (Eds.), John Wiley & Sons, Ltd., [Chichester](#), 2012.

761 Hannah, D.M., Malcolm, I.A., Soulsby, C., and Youngson, A.F.: Heat exchanges and  
762 temperatures within a salmon spawning stream in the Cairngorms, Scotland: Seasonal and sub-  
763 seasonal dynamics. *River Research and Applications*, 20, 635-652, 2004.

764 Hannah, D.M., Malcolm, I.A., Soulsby, C., and Youngson, A.F.: A comparison of forest and  
765 moorland stream microclimate, heat exchanges and thermal dynamics. *Hydrological Processes*,  
766 22, 919-940, 2008.

767 Kay, J.E., Kampf, S.K., Hancock, R.N., Cherkauer, K.A., Gillespie, A.R., and Burges, S.J.:  
768 Accuracy of lake and stream temperatures estimated from thermal infrared images. *Journal of*  
769 *the American Water Resources Association*, 41, 1161-1175, 2005.

770 Lamaro, A.A., Marinelarena, A., Torrusio, S.E., and Sala, S.E.: Water surface temperature  
771 estimation from Landsat 7 ETM+ thermal infrared data using the generalized single-channel  
772 method: Case study of Embalse del Rio Tercero (Cordoba, Argentina). *Advances in Space*  
773 *Research*, 51, 492-500, 2013.

774 Latapie, A., Camenen, B., Rodrigues, S., Paquier, A., Bouchard, J.P., and Moatar, F.: Assessing  
775 channel response of a long river influenced by human disturbance. *Catena*, 121, 1-12, 2014.

776 ~~Ledoux, E., Gomez, E., Monget, J., Viavattene, C., Viennot, P., Ducharne, A., Benoit, M.,  
777 Mignolet, C., Schott, C., and Mary, B.: Agriculture and groundwater nitrate contamination on  
778 the Seine basin. The STICS-MODCOU modelling chain. *Sciences of Total Environment*, 33-  
779 47, 2007.~~

780 Loheide, S.P. and Gorelick, S.M.: Quantifying stream-aquifer interactions through the analysis  
781 of remotely sensed thermographic profiles and in-situ temperature histories. *Environmental  
782 Science and Technology*, 40, 3336-3341, 2006.

783 Mallast, U., Cloaguen, R., Friesen, J., Rödiger, T., Geyer, S., Merz, R., and Siebert, C.: How to  
784 identify groundwater-caused thermal anomalies in lakes based on multi-temporal satellite data  
785 in semi-arid regions. *Hydrology and Earth System Sciences*, 18, 2773-2787, 2014.

786 ~~Mardhel V., Frantar P., Uhan J., and Andjelov M.: Index of development and persistence of the  
787 river networks (IDPR) as a component of regional groundwater vulnerability assessment in  
788 Slovenia. *Proceedings on the International Conference on Groundwater vulnerability  
789 assessment and mapping, Ustron, Poland, 15-18 June, 2004.*~~

790 Moatar, F. and Gailhard, J.: Water temperature behaviour in the river Loire since 1976 and  
791 1881. *Surface Geosciences*, 338, 319-328, 2006.

792 Monk, W.A., Wilbur, N.M., Curry, R.A., Gagnon, R., and Faux, R.N.: Linking landscape  
793 variables to cold water refugia in rivers. *Journal of Environmental Management*, 1, 170-176,  
794 2013.

Mis en forme : Anglais (États-Unis)

795 Monteil, C.: Estimation de la contribution des principaux aquifères du bassin versant de la Loire  
796 au fonctionnement hydrologique du fleuve à l'étiage. Ph.D. thesis, Mines Paris Tech, Paris,  
797 France, 2011.

798 [Pryet, A., Labarthe, B., Saleh, F., Akopian, M., and Flipo, N.: Reporting of stream-aquifer flow](#)  
799 [distribution at the regional scale with a distributed process-based model, Water Resources](#)  
800 [Management, 29, 139-159, 2015.](#)

801 ~~Putot, E. and Bichot, F.: CPER 2000-2006 Phase 4 — Modèle Infra-Tertiaire Dogger : calage~~  
802 ~~du modèle hydrodynamique en régime transitoire. BRGM, Orléans, France, Rep. BRGM/RP~~  
803 ~~55742-FR, 2007.~~

804 Quintana-Segui, P., Moigne P.L., Durand Y., Martin E., Habets, F., Baillon, M., Canellas, C.,  
805 Franchisteguy, L., and Morel, S.: Analysis of near surface atmospheric variables: Validation of  
806 the SAFRAN analysis over France. Journal of Applied Meteorology and Climatology, 47, 92-  
807 107, 2008.

808 Robinson, I.S., Wells, N.C., and Charnock, H.: The sea surface thermal boundary layer and its  
809 relevance to the measurements of sea surface temperature by airborne and spaceborne  
810 radiometers. International Journal of Remote Sensing, 5, 19-45, 1984.

811 [Rushton, K.: Representation in regional models of saturated river-aquifer interaction for](#)  
812 [gaining-losing rivers, Journal of Hydrology, 334, 262-281, 2007.](#)

813 [Saleh, F., Flipo, N., Habets, F., Ducharne, A., Oudin, L., Viennot, P., Ledoux, E.: Modeling the](#)  
814 [impact of in-stream water level fluctuations on stream-aquifer interactions at the regional scale,](#)  
815 [Journal of Hydrology, 400, 490-500, 2011.](#)

816 Salençon, M.J. and Thébaud, J.M.: Modélisation d'écosystème lacustre. Masson (Eds.), Paris,  
817 France, 1997.

Mis en forme : Anglais (États-Unis)

818 [Schomburgk, S., Brugeron, A., Winckel, A., Ruppert, N., Salquebre D., and Martin, J.C.:](#)  
819 [Contribution des principaux aquifères au fonctionnement hydrologique de la Loire en région](#)  
820 [Centre – Caractérisation et bilans par bassins versants souterrains, BRGM, Orléans, France,](#)  
821 [Rep. BRGM/RP 60381-FR, 2012.](#)

822 Smikrud, K.M., Prakash, A., and Nichols, J.V.: Decision-based fusion for improved fluvial  
823 landscape classification using digital aerial photographs and forward looking infrared images. *Photogrammetry and Remote Sensing*, 74, 903-911, 2008.

824

825 Sophocleous, M.: Interactions between groundwater and surface water: the state of science. *Hydrogeology Journal*, 10, 52-67, 2002.

826

827 Tonolla, D., Acuna, V., Uehlinger, U., Frank, T., and Tockner, K.: Thermal heterogeneity in  
828 river floodplains. *Ecosystems*, 13, 727-740, 2010.

829 Torgersen, C.E., Price, D.M., Li, H.W., and McIntosh, B.A.: Multiscale thermal refugia and  
830 stream habitat associations of Chinook salmon in northeastern Oregon. *Ecological*  
831 *Applications*, 9, 301-319, 1999.

832 Torgersen, C.E., Faux, R.N., McIntosh, B.A., Poage, N.J., and Norton, D.J.: Airborne thermal  
833 remote sensing for water temperature assessment in rivers and streams. *Remote Sensing of*  
834 *Environment*, 76, 386-398, 2001.

835 [US Geological Survey: Landsat-A Global Land-Imaging Mission, US Geological Survey Fact](#)  
836 [sheet, Sioux Falls, Dakota, USA, p. 4, 2012, revised: 30 May 2013.](#)

837 [USGS.: Landsat fact sheet. 2013.](#)

838 Wang, L.T., McKenna, T.E., and DeLiberty, T.L.: Locating ground-water discharge areas in  
839 Rehoboth and Indian River bays and Indian River, Delaware, using Landsat 7 imagery. *Report*  
840 *of investigation no. 74.* Delaware geological survey, [Newark, State of Delaware, USA,](#) 2008.

Mis en forme : Police :(Par défaut) Times New Roman,  
12 pt, Couleur de police : Noir

841 Ward, J.V.: Aquatic Insect Ecology, Part I, biology and habitat. Wiley & Son (Eds.), New  
842 York, USA. 1992.

843 Wawrzyniak, V.: Etude multi-échelle de la température de surface des cours d'eau par imagerie  
844 infrarouge thermique: exemples dans le bassin du Rhône. Ph.D. thesis, Université Jean-Moulin,  
845 Lyon, France, 2012.

846 Wawrzyniak, V., Piégay, H., and Poirel, A.: Longitudinal and temporal thermal patterns of the  
847 French Rhône River using Landsat ETM+ thermal infrared (TIR) images. Aquatic Sciences,  
848 74, 405-414, 2012.

849 Wawrzyniak, V., Piégay, H., Allemand, P., Vaudor, L., and Grandjean, P.: Prediction of water  
850 temperature heterogeneity of braided rivers using very high resolution thermal infrared (TIR)  
851 images. International Journal of Remote Sensing, 34, 4812-4831, 2013.

852 Webb, B.W. and Zhang, Y.: Spatial and seasonal variability in the components of the river heat  
853 budget. Hydrological Processes, 11, 79-101, 1997.

854 Webb, B.W. and Zhang, Y.: Water temperatures and heat budgets in Dorset chalk water  
855 courses. Hydrological Processes, 13, 309-321, 1999.

Mis en forme : Anglais (États-Unis)

Mis en forme : Police : (Par défaut) Times New Roman,  
12 pt, Couleur de police : Noir

Mis en forme : Anglais (États-Unis)

Mis en forme : Anglais (États-Unis)

Mis en forme : Anglais (États-Unis)

856 Table 1. Loire River temperature, air temperature and river flow rate at the date and hour-time  
 857 when satellite images were taken.

Code de champ modifié

Date	Daily river flow in Orléans (m <sup>3</sup> /s)	Hourly mean water temperature in Dampierre (°C)	Hourly mean water temperature in Saint-Laurent des Eaux (°C)	Hourly air temperature in Orléans (°C)
Winter				
15/11/2001	182	5.2	5.875	5.65
22/02/2003	478	4.215	5.55	12.765
Summer				
29/05/2003	898.6	22.85	20.105	25.55
19/07/2010	112	23.4	23.1	28.325
20/08/2010	787.9	21.8	20.95	28.329
24/08/2000	83.3	24.0	22.55	30.45
29/07/2002	61.1	28.3	26.0	32.5

Mis en forme : Exposant

858

Table 2. Details of the atmospheric heat fluxes calculations.

Solar radiation	RS estimated from the SAFRAN database	
Atmospheric radiation	$RA = \sigma_a (T_a + 273.15)^4 (A + 0.031 \cdot \sqrt{e_a}) (1 - R_L)$	<p><math>T_a</math> (°C) is the air temperature estimated from the SAFRAN database from Météo France</p> <p><math>\sigma_a = 4.9 \cdot 10^{-3} J \cdot m^{-2} \cdot d^{-1} \cdot K^{-4}</math> is the Stefan-Boltzman constant</p> <p><math>A = 0.6</math> <math>R_L = 0.03</math> are attenuation and reflection coefficients</p> <p><math>e_a = 1.22 \cdot Q_a</math> is the air vapour pressure</p> <p><math>Q_a</math> in <math>g \cdot kg^{-1}</math> is the air-specific humidity of air estimated from the SAFRAN database</p>
Emitted radiation	$RE = \varepsilon \cdot \sigma_w (T_w + 273.15)^4$	<p><math>\varepsilon = 0.98</math> is the water emissivity</p> <p><math>T_w</math> (°C) is the mean water temperature on the section estimated from the longitudinal thermal temperature longitudinal profiles</p>
Conduction	$CV = \rho_a \cdot C_a \cdot e(V) \cdot (T_w - T_a)$	<p><math>\rho_a = 1.293 \cdot \left(\frac{273.15}{T}\right)</math> air density in <math>kg \cdot m^{-3}</math> is the function of air temperature T (K) estimated from the SAFRAN database</p> <p><math>C_a = 1002 J \cdot kg^{-1} \cdot C^{-1}</math> is the air-specific heat of air</p> <p><math>e(V) = 0.0025 \cdot (1 + V_2)</math> is the function of the wind 2 m above the ground <math>V_2</math> (<math>m^3 \cdot s^{-1}</math>)</p> <p><math>V_2 = V_{10} \cdot \left(\frac{2}{10}\right)^{0.11}</math> is used to estimate the wind 2 m above the ground as a function of the wind 10 m above the ground, itself estimated from the SAFRAN database</p>
Condensation / Evaporation	$CE = L(T_w) \cdot \rho_a \cdot e(V) \cdot (Q_w - Q_a)$	<p><math>L(T_w) = (2500.9 - 2.365 \cdot T_w) \cdot 10^3 J \cdot kg^{-1}</math> is the latent evaporation heat</p>

Mis en forme : Anglais (États-Unis)

Mis en forme : Anglais (États-Unis)

Mis en forme : Anglais (États-Unis)

Mis en forme

Mis en forme : Anglais (États-Unis)

Mis en forme

Mis en forme : Anglais (États-Unis)

Mis en forme : Anglais (États-Unis)

Mis en forme : Anglais (États-Unis)

Mis en forme : Anglais (États-Unis)

Mis en forme

Mis en forme : Anglais (États-Unis)

Mis en forme : Anglais (États-Unis)

Mis en forme : Anglais (États-Unis)

Mis en forme : Anglais (États-Unis)

Mis en forme

Mis en forme : Surlignage

Mis en forme

Mis en forme : Anglais (États-Unis)

Mis en forme

Mis en forme : Anglais (États-Unis)

Mis en forme : Anglais (États-Unis)

Mis en forme : Anglais (États-Unis)

Mis en forme

Mis en forme

Mis en forme



		$Q_w = \frac{4.596 \cdot e^{\frac{237.3 \cdot T_w}{237.3 + T_w}}}{1.22}$ <p><math>Q_w</math> in <math>g \cdot kg^{-1}</math> is the specific humidity of the saturated air at the -water temperature</p>
--	--	--

Mis en forme : Anglais (États-Unis)

Mis en forme : Anglais (États-Unis)

Mis en forme : Anglais (États-Unis)

861 Table 3. Standard deviation of water temperature (°C) estimated on all the 200-m sections of  
 862 the Loire River. ~~Standard deviations were~~ is calculated at sections with ~~either~~ under 20 water  
 863 pixels ~~in the section~~ and/or over 20 water pixels. ??

Date	24/08/2000	15/11/2001	29/07/2002	22/02/2003	29/05/2003	19/07/2010	20/08/2010
$\sigma$ (n<20)	<u>0.70</u>	0.56	0.76	0.32	0.45	0.42	0.52
$\sigma$ (n>20)	<u>0.50</u>	0.44	0.73	0.26	0.41	0.41	0.42

Mis en forme : Anglais (États-Unis)

Mis en forme : Non Surlignage

Mis en forme : Anglais (États-Unis)

Mis en forme : Anglais (États-Unis)

Mis en forme : Anglais (États-Unis)

864

865

866 Figure 1. Map of the study area. The delineation of the Beauce aquifer comes from the BDLISA  
867 database from the Bureau de Recherches Géologiques et Minières (BRGM).

Mis en forme : Anglais (États-Unis)

868

869 Figure 2. Differences between TIR derived temperatures extracted from the longitudinal  
870 temperature profile and *in situ* measurements (at the same date and ~~hour~~time) at for each date.  
871 The dates are classified according to the air temperature at the time when the images ~~are~~were  
872 taken (air temperature ~~rises~~rose from ~~the~~-15/11/2001 to ~~the~~-29/07/2002).

Mis en forme : Anglais (États-Unis)

Mis en forme : Police :Italique

873

874 Figure 3. ~~Loire temperature profiles in summertime. For each profile data were centered, so that~~  
875 ~~the average temperature appears to be 0°C~~ A: ~~Relationship between the temperatures extracted~~  
876 ~~from the non-pure water pixels and the temperatures extracted those from the pure water pixels.~~  
877 ~~Temperature values of both pixel types were averaged over the successive 200-m sections~~  
878 ~~where pure water pixels existed. Summer temperatures are represented. B: Relationship~~  
879 ~~between the temperatures extracted from the non-pure water pixels and the temperatures~~  
880 ~~extracted from the pure water pixels. The temperatures values of both pixel types were~~  
881 ~~averaged over the successive 200-m sections where pure water pixels existed. Winter~~  
882 ~~temperatures are represented.~~

Mis en forme : Anglais (États-Unis)

883

884 Figure 4. A: Loire temperature profiles in winter ~~time extracted from the TIR images. For each~~  
885 ~~profile data were centered, so that the average temperature appears to be 0°C.~~ B: Loire  
886 temperature profiles in summer ~~time~~ extracted from the TIR images. For each profile data were  
887 centered.

Mis en forme : Anglais (États-Unis)

888

889 Figure 5. A: Groundwater discharge per sections of the Loire River estimated at the different  
890 dates using the heat budget based on the TIR images (black points), and calculated by ~~the~~  
891 groundwater ~~budget method~~modeling (~~grey triangles~~grey line), as a function of the river  
892 kilometers. B: Absolute value of the difference between groundwater discharges estimated by  
893 groundwater modeling and ~~with~~the heat budget.

Mis en forme : Anglais (États-Unis)

894

895 Figure 6. A: Calculated groundwater discharge along the Loire River in 20/08/2010 using  
896 groundwater modeling and the heat budget. B: Calculated groundwater discharge along the  
897 Loire River in 15/11/2001 using groundwater modeling and the heat budget.

898

899 Figure ~~67~~. Groundwater discharge rate as a function of the variation in river flow in the 48 h  
900 ~~preceding the taking of before~~ the TIR image ~~was taken~~.

901

902 Figure ~~78~~. Temperatures measured in the Loire River in the vicinity of La Chapelle Saint-  
903 Mesmin on the 29/07/2002. Groundwater discharge is visible along the right bank (north side)  
904 of the Loire River as a cold patch between river kilometers 642 and 644.

905

Mis en forme : Anglais (États-Unis)

Mis en forme : Anglais (États-Unis)

Mis en forme : Anglais (États-Unis)

Mis en forme : Anglais (États-Unis)

906 **Answer to Reviewers**

907

908 The line numbers mentioned correspond to the line numbers of the revised manuscript (not of  
909 the marked-up manuscript).

910

911 **Response to reviewer 1 :**

912

913 1. “Quantification of the Beauce’s Groundwater Contribution to the Loire River  
914 Discharge Using Satellite Infrared Imagery” uses Landsat TIR images to  
915 determine groundwater contributions to the Loire River using a simple energy  
916 budget approach and compares this to a groundwater budget approach. A  
917 method for determining groundwater contributions to rivers over space and time  
918 is presented, however there were many different assumptions and  
919 acknowledged errors in data utilized, calculations completed, or comparisons  
920 made that undermine the potential impact of the study. “

921 Despite the uncertainties, this study shows that extracted temperature profiles nevertheless  
922 remain in agreement with known areas of groundwater discharge along the Loire River.

923 A quantification of the uncertainty associated to the heat budget method has been added to the  
924 revised version of the manuscript (part 3.5 – revised manuscript). We show that uncertainties  
925 are not very likely to undermine the major findings of this study.

926 We also choose to present in the revised version of the manuscript a deterministic process-based  
927 hydrogeological model of the Loire River basin (part 3.4 – revised manuscript). This model  
928 allows the quantification of the daily groundwater discharge along the Loire River. It is  
929 therefore better suited to the comparison with the heat budget than the groundwater budget  
930 previously used. We find that both methods (groundwater budget and hydrogeological model)  
931 give similar results and that they are in agreement with the heat budget.

932

933 2. Number of pixels spanning the channel that were included within the analysis.  
934 In general, there were 3 pixels spanning the channel, but at times these were  
935 mixed pixels (water and land). The mixed pixels were still included within the  
936 analysis (2053 line 3-7).

937 We do not use mixed pixels in the study (i.e. composed of land and water). All the pixels used  
938 are water pixels only. However, the number of water pixels across the stream is variable and at

939 times lower than 3. That means, we do use pixels that are not pure (i.e adjacent to mixed pixels  
940 but still composed of water only). In our terminology, pure water pixels stands for water pixels  
941 that are situated more than a pixel away from any mixed pixels. The manuscript has been  
942 clarified in this regard (lines 150-159 – revised manuscript).

943  
944 3. No atmospheric corrections of the satellite TIR (2053 line 11) and shade  
945 influences from clouds were removed (2053 line 1-2). There was no explanation  
946 of how cloud influences were removed.

947 No atmospheric corrections are done in this study. However, this is mostly an issue when  
948 considering temperature variations over distances covering several satellite images (Handcock  
949 et al., 2012). In the current study, the studied river length is only 135 km and included in a  
950 single image. The river flows over a flat landscape. On the days when the images are taken, the  
951 sky was clear over the whole area and atmospheric conditions were therefore expected to be  
952 homogeneous. Furthermore, the Loire River is discretized in sections that do not exceed 30 km  
953 in length. It is therefore expected that atmospheric influences over the infrared radiations  
954 emitted from the water do not play a significant role in explaining the temperature variations  
955 observed along each river section. A comment was added in the manuscript in this regard (lines  
956 162-164 – revised manuscript).

957 It is nevertheless true that a global shift of each Loire temperature longitudinal profile by a  
958 constant value is to be expected after taking into account atmospheric corrections (Handcock et  
959 al., 2012). However, this shift is likely to be small ( $<1^{\circ}\text{C}$ ), since the average difference between  
960 temperature measured in-situ and temperature estimated from the non-atmospherically  
961 corrected TIR images does not exceed  $1^{\circ}\text{C}$ . Overall, the error made on the groundwater  
962 discharge estimate while not taking into account atmospheric correction is therefore of the same  
963 order of magnitude as the error made while not taking into account groundwater temperature  
964 variability, i.e. 10 to 30% (see response to comment 7). The uncertainty due to the river  
965 temperature estimate has been taken into account in the calculation of the global uncertainty  
966 (part 3.5 – revised manuscript).

967 Clouds and their shades on the ground surface are detected visually using the TM8 band and  
968 the corresponding pixels from the TM6 band are removed manually from the analysis (lines  
969 145-147 – revised manuscript). Overall, clouds are few as only images with under 10% of cloud  
970 cover are selected.

971  
972 4. Tributaries and power plant influences were considered negligible even though  
973 their influence was difficult to separate (2051 line 24-25) and can be close to  
974 1\_C in the winter (2051 line 10-16).

975 No warming of the Loire River temperature was observed downstream of Dampierre and Saint-  
976 Laurent des Eaux, based on the TIR images (lines 506-512 – revised manuscript). We do not  
977 possess in-situ measurements of the water warming in the vicinity of the power stations. Reports  
978 from EDF show that, at Dampierre, in July 2010, the mean temperature increase is 0.1°C, while  
979 the maximum temperature increase is 0.18°C. Such a low temperature increase can not  
980 necessarily be identified with the satellite TIR images. EDF uses cooling towers to reduce the  
981 temperature of the water that is released into the Loire River. A 1°C maximum temperature  
982 increase was reported in winter, but only at low flow (i.e. well below 100 m<sup>3</sup>/s). Such flows  
983 were not observed during the acquisition period of the TIR images, in winter. The choice was  
984 therefore made not to take into account the influence from the power plants, as the induced  
985 water temperature changes are small.

986 It is true that influence from the tributaries was not considered in this study (lines 115-120 –  
987 revised manuscript). In the case of the main tributary, the Loiret River, its influence is not  
988 separated from that of the groundwater because it is very short in length (less than 10 km) and  
989 its water is mainly of groundwater origin. Thus, we consider the Loiret discharge as  
990 groundwater discharge. Temperature variations along the Loire River, which can be attributed  
991 to the main groundwater discharge area (close to La Chapelle Saint-Mesmin), start upstream of  
992 the confluence with the Loiret River (see Figure 7). This shows that the Loiret River is not the  
993 only reason behind the temperature variations observed around river kilometer 635. All the  
994 other tributaries have flows under 1 m<sup>3</sup>/s and temperatures close to the Loire River temperature.  
995 Their influences on the Loire River temperature profile is therefore expected to be small and  
996 were not observed on the TIR images.

997  
998 5. Weir influences along the river (2050 line 25-27) were not accounted for.

999 Weirs influences were discussed briefly in the discussion part of the manuscript (lines 513-520  
1000 – revised manuscript). Temperature differences between the 1 km upstream reach and the 1 km  
1001 downstream reach of the main weirs remain small (less than 0.1°C). It is therefore concluded  
1002 that no significant temperature change along the water course could be related to a weir, based  
1003 on the TIR images.

1004

1005 6. Surface area estimates within the heat budget calculations were based on the  
1006 pixels selected for the analysis. These did not cover the entire channel surface  
1007 area (2054 line 18-22). The potential 20% error in surface area translates into  
1008 increased error in heat budget calculations because this value scales all surface  
1009 flux estimates (S in eqn. 3).

1010 The choice was made to consider the water pixels from the TM61 band of the LANDSAT  
1011 images to estimate the Loire River surface area (lines 201-204 – revised manuscript), since we  
1012 do not possess aerial images of finer spatial resolution at the date of the satellite images. This  
1013 technique allows taking into account variations in the extent of the Loire River with time. The  
1014 error in the surface estimate we discussed about is estimated by comparing, over each Loire  
1015 River section, the area calculated using the water pixels from the TM 61 band (30 m) and the  
1016 area calculated using the TM 8 band with a better spatial resolution (15 m). A description of  
1017 this comparison has been added in the manuscript (lines 275-278 – revised manuscript). The  
1018 uncertainty due to the surface estimate has been taken into account in the calculation of the  
1019 global uncertainty (part 3.5 – revised manuscript).

1020

1021 7. Groundwater temperatures were assigned for summer and winter based on a  
1022 data base (2054 line 16). No information was provided regarding the data or  
1023 variability in these values.

1024 ADES is a French database on groundwater data. It notably gathers most of the groundwater  
1025 temperature measurements carried out by the different surveying agencies and water  
1026 companies. The temperatures are measured irregularly over time. The precision of the  
1027 temperature measurements is  $\pm 0.1^{\circ}\text{C}$ . Data from the piezometers situated close to the Loire  
1028 River is gathered for the period 1991-2011 (292 measurements). Looking at the measured  
1029 temperatures, it appears that 80% of the temperatures are comprised between  $11.5^{\circ}\text{C}$  and  $14^{\circ}\text{C}$   
1030 in summer and between  $11^{\circ}\text{C}$  and  $13.5^{\circ}\text{C}$  in winter. These details have been added in the  
1031 manuscript (lines 196-200 – revised manuscript).

1032 The influence on the computed groundwater discharge of such a variability in the groundwater  
1033 temperature can be assessed, considering that surface water temperatures varies between  $4.5^{\circ}\text{C}$   
1034 and  $6^{\circ}\text{C}$  in winter and between  $20^{\circ}\text{C}$  and  $26^{\circ}\text{C}$  in summer. Taking into account these  
1035 temperature variations, we found that the groundwater discharge can fluctuate between 90%  
1036 and 130% of the previously computed groundwater flow, based on mean groundwater  
1037 temperatures. The highest errors in the calculation of the groundwater discharge are likely to



1038 occur in winter, when the river temperature is high and when the difference between surface  
1039 water temperature and groundwater temperature is therefore low. The uncertainty due to the  
1040 groundwater temperature estimate has been taken into account the calculation of the global  
1041 uncertainty (part 3.5 – revised manuscript).

1042  
1043 8. Inaccurate estimates of river temperature from TIR when compared to river  
1044 temperatures. At times differences were  $> 3$  °C different (Figure 2) and on  
1045 average they were  $+0.3$  °C in winter and  $-1$  °C in summer (2056 line 5). Some  
1046 of the “sharp” changes in temperature used to estimate groundwater influences  
1047 were  $0.5$  °C (2057 line 19), which is a small or possibly insignificant change  
1048 relative to the errors observed. Longitudinal temperature profiles varied less  
1049 than  $2$  °C when the variability was at its highest (Figure 3).

1050 Temperature accuracy (bias) should be differentiated from temperature uncertainty (Handcock  
1051 et al., 2012). This has been clarified in the manuscript (lines 285-299 – revised manuscript).

1052 Temperature accuracy is the average difference between the temperature estimated from the  
1053 TIR images and the temperature measured in-situ. Temperature accuracy from the TIR images  
1054 is  $1^{\circ}\text{C}$  on average in summer and  $0.3^{\circ}\text{C}$  on average in winter.

1055 Temperature uncertainty is the temperature variability observed in an area that should have a  
1056 homogeneous temperature (i.e. repeatability of measurement). Temperature uncertainty is  
1057 therefore reduced, by averaging temperature over 200 m long sections and by using a moving  
1058 average to smooth the temperature profile. The study of the longitudinal evolution of the  
1059 difference between TIR images based temperature and in-situ measurements may give some  
1060 ideas about the uncertainty (lines 267-274 – revised manuscript; see Figure 2). On average, the  
1061 temperature difference variation remains below  $0.8^{\circ}\text{C}$  over the 100 km reach Dampierre –  
1062 Saint-Laurent-des-Eaux (mean variation of the temperature difference of  $0.0072^{\circ}\text{C}/\text{km}$ ). Sharp  
1063 temperature changes need to be compared with the uncertainty and not with the accuracy. The  
1064 sharpest temperature changes observed on the longitudinal profiles are comprised between  
1065  $0.04^{\circ}\text{C}/\text{km}$  and  $0.1^{\circ}\text{C}/\text{km}$  (mean of  $0.074^{\circ}\text{C}/\text{km}$ ). The sharpest temperature changes are  
1066 therefore at least one order of magnitude higher than the changes that are to be expected from  
1067 the uncertainty. They are therefore likely to be meaningful in terms of physical processes (lines  
1068 335-340 – revised manuscript).

1069  
1070 9. The overarching concern with these combined assumptions and errors are the  
1071 influences on the findings within the paper. It is unclear if there is enough

1072 variability in the longitudinal temperatures to confidently back out groundwater  
1073 influences and needs to be further investigated. There are many questions and  
1074 concerns regarding the influence of the assumptions or treatment of data. What  
1075 are the errors in the satellite based TIR data and what is the influence of not  
1076 correcting for atmospheric conditions that will vary throughout the study reach  
1077 and over different times of year? Torgersen et al. 2001 states that 10 pixels are  
1078 required to avoid the influences of banks emission and to get accurate river  
1079 temperatures. It does not seem that 3 pixels are adequate, particularly when  
1080 they are mixed pixels. Given these issues and additional uncertainty in other  
1081 foundational data used in the heat balance approach (e.g., assumed  
1082 groundwater temperature and incorrect surface area estimates), the confidence  
1083 in groundwater estimates are likely low.

1084 We previously discussed the influence atmospheric corrections would have on our study. It  
1085 would have an influence on the temperature accuracy but not on the temperature uncertainty.

1086 Torgersen et al. (2001) chose arbitrarily 10 pixels in each thermal image and took the median  
1087 temperature value. Temperature longitudinal profiles were then drawn using these median  
1088 values. This method can only be employed when using multiple images (mostly for airborne  
1089 campaign). However, our method is similar in that we average river temperatures by sections  
1090 of 200 m to draw the longitudinal profiles. This is a spatial extent of the same order of  
1091 magnitude as the usual ground coverage of a TIR image taken from an airborne campaign. The  
1092 advantage of our method is that we consider all the water pixels from the water course. There  
1093 could therefore be more than 10 pixels in the 200 m sections. Then, uncertainty is further  
1094 reduced through a moving average smoothing of the data over  $\pm 2$  km.

1095 We carried out sensitivity tests to estimate the overall uncertainty in our groundwater discharge  
1096 estimation using the heat budget. Details about these tests have been added in the new  
1097 manuscript (lines 373-379 – revised manuscript). One figure is added in the manuscript to show  
1098 the confidence interval of the groundwater discharge estimation at two dates, one in summer  
1099 and one in winter (Figure 6).

1100  
1101 10. The current comparison with the groundwater budget that has long averaging  
1102 times, similar uncertainties, and is vaguely described does not provide the type  
1103 of validation needed to illustrate the potential of this approach. In order for this  
1104 paper to have an impact within the remote sensing and groundwater  
1105 communities, more information regarding a quantitative understanding of the  
1106 accuracy of the proposed methodologies is necessary. Some additional  
1107 information that validate the findings is also needed.

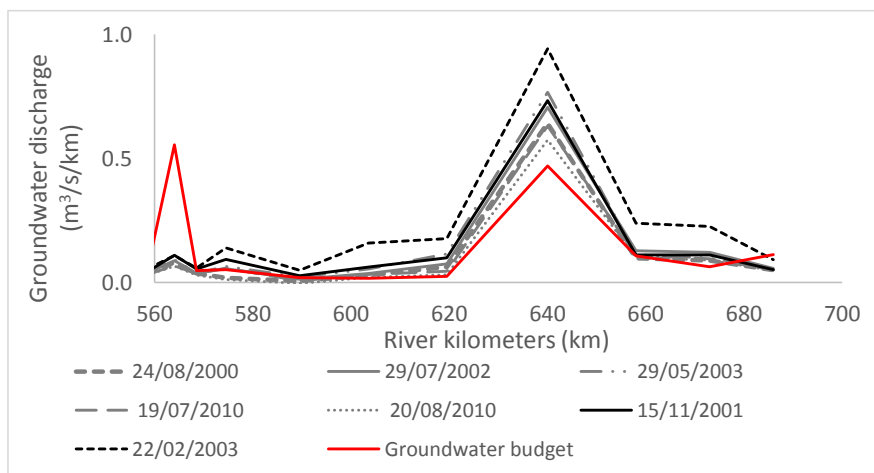
1108 To validate further the findings, we replace the groundwater discharge calculated using the  
1109 groundwater budget by the groundwater discharge calculated using a deterministic process

1110 based groundwater model over the entire Loire River basin. Using this model, the groundwater  
 1111 discharge to the Loire River can be calculated at each date and at every river kilometers.  
 1112 Uncertainty in the model prediction of the Loire River flow is known and low (Nash criteria of  
 1113 0.98). Details about the uncertainty in the groundwater discharge estimated through modeling  
 1114 have been added in the manuscript (lines 452-454 – revised manuscript). The groundwater  
 1115 model was developed by Fulvia Baratelli and Nicola Flipo. They are included in the new authors  
 1116 list of the manuscript.

1117 We found that the newly calculated groundwater discharge remains in agreement with the  
 1118 groundwater discharge previously calculated with the groundwater budget (see Figure A  
 1119 below). The highest groundwater discharges calculated by both methods are situated between  
 1120 river kilometers 620 and 660. However, on average, groundwater discharge rates calculated  
 1121 using groundwater modeling are higher than the groundwater discharge rates estimated with  
 1122 the groundwater budget. Higher groundwater discharge rates are also estimated in winter than  
 1123 in summer, which is in agreement with what was found using the heat budget. This remark has  
 1124 been added to the manuscript (lines 484-487 – revised manuscript).

1125 Two figures are added in the manuscript to show the groundwater discharge calculated by the  
 1126 groundwater model (Figure 5; Figure 6).

1127



1128

1129

1130

Figure A: Groundwater discharge estimated using a groundwater budget over successive Loire River groundwater catchment areas and using groundwater modeling over the entire Loire River basin.

1131

1132 **Response to reviewer 2 :**

1133

1134 11. This manuscript presents interesting results on how Landsat imagery in the TIR  
1135 band can be used to map water temperature in a large river synoptically over  
1136 hundreds of kilometers. This approach has been used in other large rivers, but  
1137 the Loire River is particularly interesting because it is influenced by relatively  
1138 high-volume groundwater inputs and is quite narrow (in places) for using  
1139 satellite TIR imagery. Furthermore, the seasonal differences in river  
1140 temperature provide an important perspective on thermal heterogeneity  
1141 experienced by riverine biota. The paper could significantly improve our  
1142 understanding of riverine thermal regimes and spatial patterns at broad scales,  
1143 and it could be a useful contribution to the literature on thermal remote sensing  
1144 of rivers, but unfortunately its presentation is quite poor. It is confusingly written  
1145 from the standpoint of scientific English, and its organization requires significant  
1146 revision to highlight the strengths and weaknesses of the study. For example,  
1147 the data on the accuracy assessment need to be presented in more detail. The  
1148 only data presented on the accuracy of the method are in Figure 2, which only  
1149 presents means, which are not very useful. The authors need to present box  
1150 and whisker plots perhaps to show the reader how variable the differences were.  
1151 Furthermore, the authors mention that linear regression was used to evaluate  
1152 kinetic and radiant temperatures, but these linear regressions and their statistics  
1153 are not shown or reported. It would seem that the remote sensing part of this  
1154 study would alone be a nice contribution but would require more more detail for  
1155 the reader to truly evaluate the data. I am not qualified to evaluate the methods  
1156 for estimating groundwater discharge, but it appears that this part of the  
1157 manuscript is poorly developed. The main objectives of the paper pertain to the  
1158 TIR data and how they can be used to locate thermal anomalies associated with  
1159 groundwater at different times of the year. The authors may wish to reconsider  
1160 how important the actual calculations of discharge are for this paper.

1161 Many small modifications have been made to improve the readability of the manuscript. They  
1162 have been made by an English speaking translator. The modifications are visible in the marked-  
1163 up manuscript. They do not change the aims and scope of the manuscript.

1164 Comments on the accuracy and uncertainty have been added to the manuscript (see response to  
1165 comment 1).

1166 Linear regression was not used to correct radiant temperature from in-situ measurements of  
1167 kinetic temperature. Linear regression does not work well, although radiant temperature tends  
1168 to overestimate kinetic temperature in winter and to underestimate it in summer (see Figure 2).

1169 Linear regression was used to compare, when this was possible, temperatures extracted from  
1170 the pure water pixels and temperatures extracted from the non-pure water pixels, in order to  
1171 assess the robustness of the method (see response to comment 18).

1172 We found that the calculation of the groundwater discharge is an important part of this work.  
1173 One of the findings of this study is that, despite all the uncertainties associated to the use of  
1174 satellite TIR images, the main groundwater discharge area in the Loire River can still be  
1175 identified. Moreover, the calculated groundwater flow remains credible in regard to what was  
1176 found in previous studies and to what we find using a groundwater flow budget over the  
1177 successive catchment areas and groundwater modeling. Quantification of groundwater  
1178 discharge using TIR images has already been conducted in the past (Loheide and Gorelick,  
1179 2006) but it has been used on a much smaller river. It is therefore interesting to see if Landsat  
1180 images could also be employed.

1181  
1182 12. Title: Specify "thermal IR" not just IR. Also, write out Beauce Aquifer because  
1183 most readers won't know what the "Beauce" is.

1184 The corrections have been made.

1185  
1186 13. Page 2048, Line 20: Throughout the manuscript, the authors write "Thermal  
1187 InfraRed". Just write "thermal infrared (TIR)" and use standard terminology as  
1188 in the papers that are cited in the references.

1189 The corrections have been made.

1190  
1191 14. Page 2049: Check spelling of "Burckholder". I think it doesn't have a "k". Also,  
1192 the word "evolution" doesn't make sense as it is used throughout this  
1193 manuscript.

1194 In fact, it should have been written "Burkholder". It has a "k" but no "c". The corrections have  
1195 been made. The word "evolution" was replaced by "variations".

1196  
1197 15. Page 2050: The authors need to say something about the presence of large  
1198 wood, boulders, and gravel bars because they can also be a cause for mixed  
1199 pixels, not just the banks.

1200 In the Loire River, there are no boulders, as the sediments are mostly composed of sand and  
1201 gravel. The gravel and sand bars are detected using the TM 8 band from the Landsat images.  
1202 They are considered in the same way as the river banks and pixels from TIR images are

1203 therefore discarded when overlapping sand bars. Trees in the water, as well as very small sand  
1204 bars, are not likely to be detected due to the resolution of the TM 8 band pixels (15\*15 m<sup>2</sup>  
1205 pixels). But, it is therefore assumed that these obstacles do not cover an important area within  
1206 the 60\*60 m<sup>2</sup> water pixels from the TM 6 band.

1207

1208 16. Page 2052, Line 18: This is confusing because the authors refer to the near IR  
1209 data before they even describe the TIR data from the satellite. In fact, the  
1210 authors don't identify the spatial resolution of the IR and TIR bands in the  
1211 methods. Please check your methods. They are not presented in a logical order  
1212 and they need to provide more detail.

1213 Comments have been added in the manuscript for better clarity (lines 138-159 – revised  
1214 manuscript). Resolutions of the IR and TIR bands are described.

1215

1216 17. Page 2053: The fact that the authors use data where there are only three pixels  
1217 across the width of the stream is quite surprising, given what papers have  
1218 described. It is really important for these data to be fully reported. After reading  
1219 this paper, I am somewhat convinced that < 3 pixel may work in certain  
1220 instances, but I need more data to be convinced.

1221 The choice to use all the water pixels was made since we could otherwise not have covered the  
1222 full length of the selected river reach. However, we made sure that the resulting bias was not  
1223 too important (lines 300-309 – revised manuscript).

1224

1225 18. Page 2056: Where are the results and plots for the regression analysis?

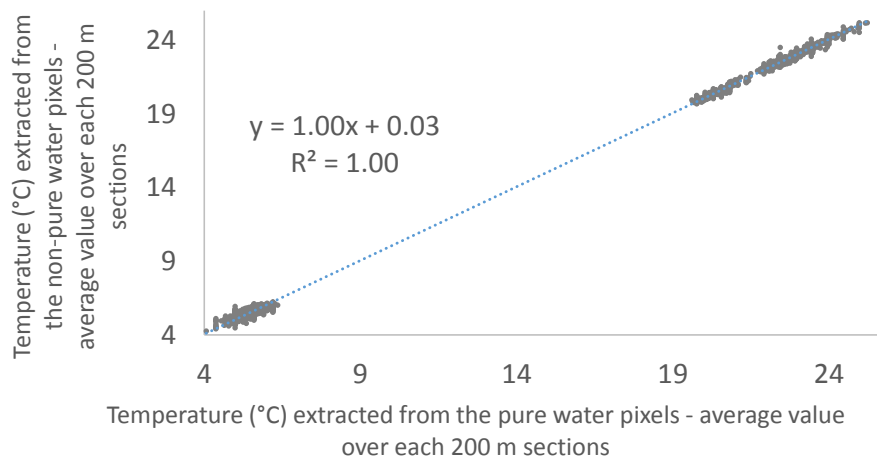
1226 We add one figure in the manuscript showing the comparison between temperatures extracted  
1227 from non-pure water pixels and temperatures extracted from pure water pixels, over all the 200  
1228 m sections of the Loire River where pure water pixels could be found (see Figure 3). We found  
1229 that there is no significant shift between temperatures extracted from pure water pixels and  
1230 temperatures extracted from non-pure water pixels. The non-pure water pixels do not  
1231 particularly overestimate the water temperature in summer (Figure 3a in the manuscript), as it  
1232 was expected from the high river banks temperatures. The slope of the regression line is 0.99  
1233 and the coefficient of determination is 0.98. In winter, a slight underestimation of water  
1234 temperature within the non-pure water pixels could be seen (Figure 3b in the manuscript), with  
1235 a slope of the regression line of 0.72. However, the coefficient of determination is quite low ( $R^2$   
1236 = 0.69) and we lack data to conclude (the range of variation of water temperature is much  
1237 smaller in winter than in summer). These results are added in the manuscript (lines 300-309 –

1238 revised manuscript). Considering both summer and winter data, the slope of the regression line  
1239 is 1 with a regression coefficient of 1 (see Figure B below).

1240 The difference between temperatures extracted from pure water pixels and from non-pure water  
1241 pixels usually remains in the  $\pm 0.5^\circ\text{C}$  interval (for over 98% of the 200 m sections). This  $0.5^\circ\text{C}$   
1242 gap corresponds to the approximate sensor resolution of the satellite camera (see Figure C  
1243 below).

1244 As we consider in our analysis both pure and non-pure water pixels, and since we use a moving  
1245 average over  $\pm 2$  km to smooth the temperature profile, we expect the bias resulting from the  
1246 use of non-pure water pixel to remain relatively low.

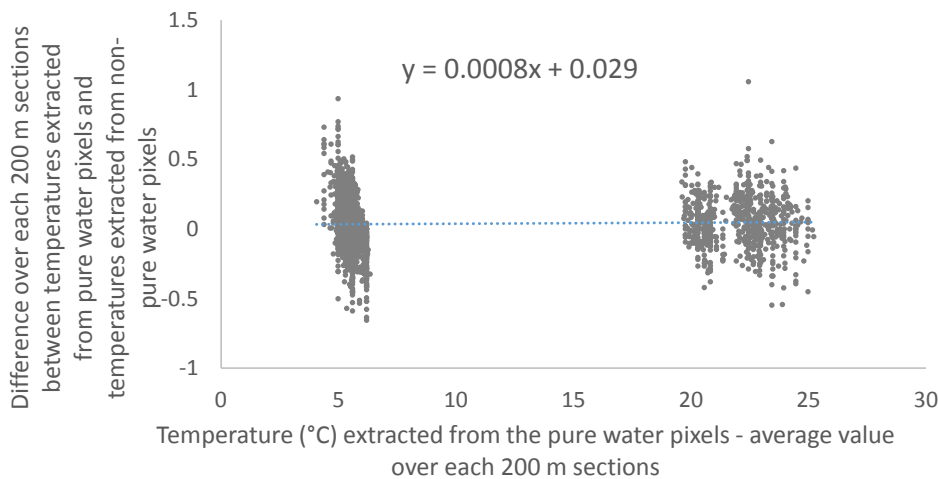
1247



1248

1249 *Figure B: Relation between the temperature extracted from the non-pure water pixels and the temperature extracted from*  
1250 *the pure water pixels. Temperature values of both pixels types are averaged over the successive 200 m sections where pure*  
1251 *water pixels exist. Both winter and summer temperature values are represented.*

1252



1253

1254 *Figure C: Difference between the temperature extracted from the pure water pixels and the temperature extracted from the*  
 1255 *non-pure water pixels. Temperature values of both pixels types are averaged over the successive 200 m sections where pure*  
 1256 *water pixels exist.*

1257

1258 19. Table 1: What time were these temperature data collected? I think it says this  
 1259 in the methods, but you should probably have it in the table as well. Standardize  
 1260 the significant digits in these numbers.

1261 The temperatures were collected at 11:30 LT in winter and 12:30 LT in summer (lines 126-127  
 1262 – revised manuscript). The significant digits have been standardized.

1263

1264 20. Table 3: Which sections? All sections? How many sections?

1265 All the 200 m sections of the Loire River are included in this analysis. The legend has been  
 1266 modified accordingly.

1267

1268 21. Figure 1: The symbols on this map are difficult to see. The triangles and the  
 1269 crosses are too faint. Also, the river km numbers need to be moved slightly so  
 1270 they are not on top of other symbols. Note that the town of Saint Laurent has a  
 1271 symbol that gets in the way of other symbols, and it is hard to read the text of  
 1272 the name. The font size is generally too small throughout this figure. Need to  
 1273 show groundtruth locations if possible. What is the light grey area? This needs  
 1274 to be stated in the caption.

1275 The map has been modified.

1276



1277 22. Figure 2: The y-axis label is too long. Shorten and provided clarification in the  
1278 text. Don't use "ones" in the label; this is not good scientific writing. Are these  
1279 mean differences? I think it would be better to have box and whisker plots of  
1280 these so you can see variation.

1281 The term "ones" has been removed from the figure.

1282 This figure shows difference between in-situ measurements of water temperatures and  
1283 temperatures estimated from the longitudinal temperature profiles obtained from the TIR  
1284 images. They are therefore a kind of mean differences. The figure caption has been modified  
1285 for better clarity.

1286 We find that box and whisker plot of the temperatures extracted from TIR images in the vicinity  
1287 of Dampierre and Saint-Laurent des Eaux would be harder to read. These box and whisker plots  
1288 show that, in most cases, the temperature measured in-situ is comprised within the range of the  
1289 temperatures observed at the neighboring water pixels from the TIR images. In these cases,  
1290 temperature discrepancies between the 2 methods could easily be explained by local  
1291 temperature heterogeneities in the water course or satellite sensor's resolution. However, there  
1292 are 3 cases where these phenomenon may not offer an adequate explanation. It occurs on the  
1293 29/05/2003 at Dampierre and on the 29/07/2002 at Dampierre and Saint-Laurent des Eaux. This  
1294 analysis is consistent with the comparison between the longitudinal temperature profiles and  
1295 the in-situ temperature measurements that is shown in the manuscript. Figure 2 was therefore  
1296 kept as it was in the revised manuscript.

1297 The discrepancies between temperatures measured in-situ and TIR images derived temperatures  
1298 are taken into account in the uncertainty analysis (lines 267-273 and 279-281).

1299  
1300 23. Figure 3: State that these are derived from satellite imagery. What does  
1301 "removed" mean in the y-axis label? Move the x-axis at the bottom of the figure.

1302 The corrections have been made.

1303  
1304 24. Figure 4: I think it would be really helpful to have Figure 3 and Figure 4 be panels  
1305 in the same figure.

1306 It has been done.

1307

1308